Publisher source acknowledgment https://doi.org/10.1016/j.ejmech.2021.114038 (final version)

Development of Novel Phenoxyalkylpiperidines as High-Affinity Sigma-1 (σ_1) Receptor Ligands with Potent Anti-Amnesic Effect

Francesca S. Abatematteo[1], Philip D. Mosier[2], Mauro Niso[1], Leonardo Brunetti[1], Francesco Berardi[1], Fulvio Loiodice[1], Marialessandra Contino[1], Benjamin Delprat[3], Maurice Tangui[3], Antonio Laghezza[1*] and Carmen Abate[1*]

[1]Dipartimento di Farmacia-Scienze del Farmaco, Università degli Studi di Bari, Via Orabona, 4, I-70125 Bari, Italy, [2]Department of Biopharmaceutical Sciences, School of Pharmacy, Medical College of Wisconsin, 8701 Watertown Plank Road, Milwaukee, WI 53226, USA, [3]MMDN, University of Montpellier, EPHE, INSERM, Montpellier, France

*Correspondence:

Carmen Abate
Tel.: +39-080-544-2751
E-mail: carmen.abate@uniba.it

Antonio Laghezza
Tel.: +39-080-544-2745
E-mail: antonio.laghezza@uniba.it

ABSTRACT: The sigma-1 (σ_1) receptor plays a significant role in many normal physiological functions and pathological disease states, and as such represents an attractive therapeutic target for both agonists and antagonists. Here, we describe a novel series of phenoxyalkylpiperidines based on the lead compounds 1-[ω-(4-chlorophenoxy)ethyl]-4-methylpiperidine (**1a**) in which the degree of methylation at the carbon atoms *alpha* to the piperidine nitrogen was systematically varied. The affinity at σ_1 and σ_2 receptors and at Δ^8-Δ^7 sterol isomerase (SI) ranged from subnanomolar to micromolar K_i values. While the highest-affinity was displayed at the σ_1, the increase of the degree of methylation in the piperidine ring progressively decreased the affinity. The subnanomolar affinity **1a** and 1-[ω-(4-methoxyphenoxy)ethyl]-4-methylpiperidine (**1b**) displayed potent anti-amnesic effects associated with σ_1 receptor agonism, in two memory tests. Automated receptor–small-molecule ligand docking provided a molecular structure-based rationale for the agonistic effects of **1a** and **1b**. Overall, the class of the phenoxyalkylpiperidines holds potential for the development of high affinity σ_1 receptor agonists, and compound **1a**, that appears as the best in class (exceeding by far the activity of the reference compound PRE-084) deserves further investigation.

KEYWORDS: sigma-1 receptor activation, sigma-1 receptor agonist, structure–affinity relationship (SAfiR), structure–activity relationship (SAR), sterol isomerase ligand, molecular modeling, learning, memory

INTRODUCTION

The sigma (σ) receptors, which were first described in 1976 as opioid receptors,[1] were later recognized as two distinct subtypes, namely σ_1 and σ_2. Four decades after their discovery, structural and functional aspects of these two intriguing receptor subtypes still require elucidation.[2] Compared to the σ_1 subtype, which was cloned in 1996[3] and structurally characterized in 2016,[4] knowledge regarding the σ_2 subtype has relied for decades on a pharmacological, rather than structural, characterization. Only recently, after some controversy,[5-8] was the σ_2 receptor unequivocally identified as the TMEM97 protein,[9] prompting novel research and further rejuvenating interest in this target within several pathological contexts.[10-13] On the other hand, knowledge about the σ_1 protein is more extensive but not yet complete. The protein has been co-crystallized with structurally and functionally divergent ligands and the receptor–ligand complexes structurally characterized by X-ray diffraction (XRD).[4,14] From these groundbreaking studies, the σ_1 receptor was shown to have a particular fold consisting of a β-barrel (with a largely hydrophobic interior where small-molecule ligands can bind) surrounded by several α-helices, two of which (α4 and α5) are accessible by ligands bound within the β-barrel and one of which (α1) is membrane-spanning and anchors the receptor to the lipid membrane.[4,14] The crystal structures have furnished insights on how the σ_1 agonists and antagonists stabilize different receptor conformations. In particular, the binding of σ_1 agonists like (+)-pentazocine results in a movement of the α4 helix away from the α5 helix, which can potentially modulate homomeric and heteromeric σ_1 protein–protein interactions (PPI) and thus σ_1 receptor function.[14]

The σ_1 receptor is a ligand-operated endoplasmic reticulum (ER)-resident protein highly concentrated at mitochondria-associated ER membranes (MAMs),[15,16] where it modulates inter-organelle exchanges such as calcium transfer in the ER stress response. It has been more recently defined as a ‘pluripotent chaperone’ that binds and modulates a wide variety of client proteins and is therefore involved in a variety of functions.[12,17] Highly expressed in the CNS, the σ_1 receptor has been shown to stimulate dendritic spine formation, modulate the microglial response to stress[18] and

regulate brain neurotransmission and plasticity pathways.[19-22] In turn, σ_1 receptor ligands are potent antidepressant and anti-amnesic ligands in different pharmacological and pathological models of learning deficits.[23] Some σ_1 receptor agonists are also neuroprotective in preclinical models of neurodegenerative diseases, including Alzheimer's disease (AD), Parkinson's disease (PD), Huntington's disease (HD), amyotrophic lateral sclerosis (ALS) and multiple sclerosis (MS).[24] For instance pridopidine, one of the most promising and highly selective σ_1 agonists, was recently shown to induce beneficial effects in ALS and HD models, with encouraging data from a clinical trial (PRIDE-HD) for the treatment of HD.[25-29] An additional role has also been described for σ_1 in the oncology field as it regulates cell proliferation, with σ_1 antagonists exerting a cytotoxic effect.[30] Importantly, σ_1 has been described as a key host dependency factor critical for SARS-CoV-1 and SARS-CoV-2 infection[31,32] and an interesting review links the antiviral activity of several investigated molecules against viruses, such as Epstein–Barr virus (EBV), hepatitis C virus (HCV) and Ebola virus, with their interaction with the σ_1 receptor.[33] Nevertheless some confounds have been revealed that may have affected the evaluation of the antiviral activity of the σ receptor ligands *in vitro*.[34] Altogether, these pieces of evidence demonstrate that important and varied therapeutic potentials are linked to σ_1 receptor modulation. Indeed, the σ_1 pharmacophore is beginning to be exploited for multi-target strategies.[35,36]

In our search for high-affinity σ_1 receptor ligands, we have identified 4-methylpiperidine as a chemotype that confers a potent binding to the receptor when linked through a 3- to 4-methylene chain to a hydrophobic portion such as tetralin/naphthalene nuclei or phenoxy rings.[37,38] While initial studies led us to hypothesize opposing functional behaviors for the tetralin-bearing compounds such as PB190 (σ_1 receptor agonists) and the naphthalene-bearing compounds such as PB212 (σ_1 receptor antagonists),[37] later studies contradicted this hypothesis (Figure 1).[39] It is worth noting that the concept of "agonist" *versus* "antagonist" for σ_1 receptor ligands is quite elusive, as agonism involves ligand-induced allosteric modulation of protein–protein interactions between the σ_1 receptor and its client proteins, and assays that can predict such interactions are under development.[40] In our recent

investigation in which novel PB212 derivatives were docked to an antagonized σ_1 receptor, comparison of structurally diverse piperidine analogs attached to the hydrophobic 6-methoxynaphthalenylbutyl portion of PB212 suggested that the steric demands of the piperidine analog (and its substituents) and that of the secondary hydrophobic site may indirectly impact the interaction of the attached hydrophobic portion with the α4 helix situated adjacent to the primary hydrophobic region of the receptor.[41] Therefore, we have built a novel small series of methyl piperidines linked by an ethylene or propylene linker to either a *para*-chlorophenoxy or a *para*-methoxyphenoxy fragment as the primary (larger) hydrophobic moiety (Table 1), on the basis of the lead compound **1a** that is characterized by sub-nanomolar σ_1 receptor affinity and 278-fold σ_1 *versus* σ_2 selectivity (Table 2).[38] While the *p*-chlorophenoxy moiety was previously shown to be the optimal hydrophobic portion for interaction with σ_1 in a previous series of compounds, the position of the methyl group(s) on the piperidine ring has not been systematically explored. With this novel series of compounds, we have thus explored (using competition binding assays and molecular modeling techniques) how methyl groups on the piperidine ring and the presence of either *p*-chloro or *p*-methoxy groups on the phenoxy moiety may impact the σ_1 binding and receptor conformation, with particular focus on the α4 helix movement that is associated with σ_1 agonist activity.

All newly-synthesized compounds were evaluated in radioligand binding assays for σ_1 and σ_2 receptors and in a Δ^8-Δ^7 sterol isomerase (SI) activity assay.[42] SI is also known as emopamil binding protein (EBP), which belongs to the EXPERA (EXPanded EBP superfamily) domain superfamily together with σ_2/TMEM97, and whose EXPERA domain structure containing four transmembrane regions is presumably like that of σ_2/TMEM97. Additionally, the lead *p*-chloro derivative **1a** and its *p*-methoxy counterpart **1b** with similar sub-nanomolar σ_1 affinity (**1a**: K_i = 0.86 nM; **1b**: K_i = 0.89 nM) and σ_1- *versus* σ_2-selectivity (**1a**: 278-fold; **1b**: 191-fold) were evaluated in the dizocilpine-induced model of amnesia in mice, a σ_1 receptor-mediated behavioral response. The tested compounds showed anti-amnesic properties that were comparable, for **1b**, or 30-fold more potent, for **1a**, than the reported activity of the reference compound PRE-084.[23,43,44] The anti-amnesic property

of σ_1 receptor ligands is linked to their agonist activity at the receptor, which was confirmed by a blockade of their behavioral effects by the σ_1 receptor antagonist NE-100, but also by the lack of cytotoxic activity of **1a** and **1b** in a panel of cancer cell lines.

RESULTS AND DISCUSSION

Chemistry. Three routes were employed to prepare the present series of phenoxyalkylpiperidines (Schemes 1–3). Compounds **1b**, **3a**,**b** and **4a**,**b** were prepared (Scheme 1) starting from the reaction between the suitable phenol and 2-chloroethanol or 3-chloropropanol that yielded the corresponding phenoxyalcohols, which were transformed into the corresponding mesylates and tosylates (**7a**,**b** and **8a**,**b**), respectively. Reaction of these compounds with the corresponding piperidines gave the desired amines **1b**, (*R*)-**3a**,**b**, (*S*)-**3a**,**b** and **4a**,**b**.

For the preparation of phenoxyalkylpiperidines (*R*)-**2b** and (*S*)-**2b**, a different synthetic approach was followed (Scheme 2). The key step of this pathway was the preparation of phthalimidoalcohol intermediates from the commercially available enantiomers of alaninol. A Mitsunobu condensation of these intermediates with 4-methoxyphenol gave the optically active intermediate phthalimidoalcohols whose hydrazinolysis yielded the phenoxyalkylamines (*R*)-**9** and (*S*)-**9**. A treatment with 3-methylglutaric anhydride, prepared *in situ*, and acetyl chloride provided the enantiomeric couple of piperidindione derivatives which were readily reduced with borane-methyl sulfide to give the desired amines (*R*)-**2b** and (*S*)-**2b**.

Compounds **5a**,**b** and **6a**,**b** were prepared starting either from the commercially available acid **10a** or from **10b**, which was readily prepared by condensation of 4-methoxyphenol with ethyl bromoacetate followed by alkaline hydrolysis. Both acids **10a** and **10b** were reacted with *cis*-2,6-dimethylpiperidine or 2,2,6,6-tetramethylpiperidine to give the corresponding amides which were readily reduced to amines with borane-methyl sulfide complex affording the target compounds (Scheme 3).

Receptor Binding Studies. The affinity values of novel and reference compounds at σ_1, σ_2 and SI sites from radioligand binding assays are reported in Table 2. The 4-methyl substituent on the piperidine ring was confirmed to confer optimal interaction with the σ_1 subtype with data from *N*-[(4-methoxyphenoxy)ethyl]piperidines **1b**, (*R*)-**2b**, (*S*)-**2b** (K_i = 0.89–1.49 nM), matching the results from their *p*-chlorophenoxy counterparts **1a**, (*R*)-**2a** and (*S*)-**2a** (K_i = 0.34–1.18 nM). A more than 10-fold reduction in the affinity was recorded for all 2-methyl, 2,6-dimethyl and 2,2,6,6-tetra-methyl *N*-[(4-chlorophenoxy)ethyl]piperidines (*R*)-**3a**, (*S*)-**3a**, **5a** and **6a** (K_i values > 16 nM) and *N*-[(4-methoxyphenoxy)ethyl]piperidines (*R*)-**3b**, (*S*)-**3b**, **5b** and **6b** (K_i values > 39 nM). In particular, the tetramethyl-substituted compounds from each series (**6a** and **6b**) did not bind the σ_1 receptor (K_i values > 5000 nM), in agreement with previous studies in which increasing the degree of steric hindrance around the basic nitrogen atom decreases the σ_1 receptor affinity.[39] Elongation of the linker from oxyethylene to oxypropylene led to a more than 10-fold increase in the σ_1 receptor affinity in the 2,6-dimethyl substituted derivatives **4a** (K_i = 4.43 nM) and **4b** (K_i = 23.5 nM), compared to their inferior homologues **5a** (K_i = 59.4 nM) and **5b** (K_i = 379 nM). Overall, while high-affinity and selective ligands were obtained in both series, each *p*-chloro derivative slightly exceeded its *p*-methoxy counterpart in σ_1 receptor affinity, with a greater beneficial effect of the more hydrophobic Cl-atom when the piperidine N-atom is more hindered. Moderate to low σ_2 receptor affinities were recorded (K_i values = 52.3–809 nM), except for compound **4a** (K_i = 17.2 nM), confirming the phenoxy portion connected to the piperidine basic moiety as an optimal scaffold to select σ_1 over σ_2 receptor binding.

For the SI site, the *N*-[(4-methoxyphenoxy)ethyl]piperidines clearly demonstrated a reduction in the affinity compared to the *p*-chloro series in which high-affinity SI ligands were included (K_i < 5 nM: **1a**, (*S*)-**2a**, (*S*)-**3a**, **5a**), resulting in generally greater σ_1 *versus* SI selectivity for members of the *p*-methoxy series.

As far as stereochemistry is concerned, little or moderate differences in the affinities between the enantiomeric pairs were observed. However, the presence of a chiral center on the ethylenic chain

seems to exert a stronger influence on the affinity compared to the presence on the piperidine ring. In fact, the highest eudismic ratios (e.r.) were shown from **2b** whose *R* enantiomer showed a 4-fold higher affinity than the corresponding *S* isomer towards σ_2 and from the previously published[38] **2a** (*R* > *S* towards σ_2, e.r. 3.5; *S* > *R* towards σ_1 and SI, e.r. 3 and 6, respectively). However, on the whole, these results confirm that more stringent structural requirements are needed for the σ_2 site in comparison to σ_1 and SI.

***In vitro* and *in vivo* studies.** Because of their excellent σ_1 receptor binding profile and lack of chirality that could complicate the pharmacokinetics, we selected the lead compound **1a** and its methoxy counterpart **1b** to be tested for anti-amnesic efficacy. While all the novel compounds were devoid of cytotoxic activity in rat C6 glioma cells, prior to the *in vivo* tests, the cytotoxicity of **1a** and **1b** was also evaluated in a panel of cancer cell lines (human neuroblastoma SK-SY5Y, hepatic adenocarcinoma HepG2, breast adenocarcinoma MCF7, Table 3) suggesting the lack of toxic activity. In general, σ_1 receptor ligands referred to as agonists are devoid of cytotoxic activity in cancer cells, and neither of the two compounds tested were cytotoxic, indicating that they function as σ_1 receptor agonists. Accordingly, we expected that our σ_1 receptor agonists should produce anti-amnesic effects when evaluated by using two complementary behavioral tests, namely spontaneous alternation in the Y-maze (measuring spatial working memory) and a step-through-type passive avoidance response (measuring non-spatial long-term memory).[43-45] Learning deficits were induced in mice (12 per group) by administering the noncompetitive NMDA receptor antagonist dizocilpine ((+)-MK-801 maleate) at a dose of 0.15 mg/kg intraperitoneally (ip) 20 min before the Y-maze test session or the acquisition session in the passive avoidance test.[43,45] The test compounds were injected ip 10 min before dizocilpine.[43,45] While **1a** administration led to attenuation of dizocilpine-induced learning deficits in the 0.03–0.3 mg/kg dose range in both tests, **1b** was effective in the 1-10 mg/kg dose range (Figure 2A,B,C,D). Administration of the σ_1 receptor antagonist NE-100 completely reverted the effect of the most active dose for each ligand, demonstrating that their anti-amnesic action occured via σ_1 receptors (Figure 2E,F). Altogether, compound **1b** is as potent as the reference compound PRE-

084,[45] while **1a** is around 30-fold more potent than PRE-084 (Figure 1), deserving further investigation in other *in vivo* models of pathologies for which σ_1 receptor agonists are beneficial.

Molecular modeling. The σ_1 ligand binding pocket is described by a β-barrel-like structure flanked on one side by two α-helices (α4 and α5), and its interior is lined with many bulky hydrophobic amino acid residues. A glutamate residue (E172), stabilized by Y103 on one side and a neutral aspartic acid (D126) on the opposite side, divides the ligand binding site into three distinct regions: 1) an amine (ammonium) binding site directly adjacent to glutamate E172 (facilitates salt bridge/H-bond interactions) and F107 (facilitates π-cation interactions), 2) a large primary hydrophobic region bounded in part by Y103 and the α4 and α5 helices, and 3) a smaller secondary hydrophobic binding region near D126, the putative entrance and "lid" of the receptor (see Figure 3).[4,14] The overall shape and electrostatic character of the binding site allows for the high-affinity binding of a large and structurally diverse family of amine-containing compounds with bulky or elongated hydrophobic substituents, as typified in the Glennon pharmacophore.[41] An outward movement of α4 away from α5, resulting in a reduction in the degree of receptor homo-trimerization, has been proposed as an activation mechanism for σ_1, and that ligands such as (+)-pentazocine that possess σ_1 agonist activity do so because they are able to induce and/or maintain this trimer-destabilizing α4 movement.[14]

To better understand how ligands like **1a** and **1b** bind to the σ_1 receptor to exert their agonist activity, a series of reference ligands (five co-crystallized ligands, PB190 and PB212, Figure 1) and the target compounds listed in Table 2 were docked to the PD144418-antagonized and (+)-pentazocine-agonized conformations of the receptor (see Experimental Methods). It has been observed in crystal structures that antagonists bind to the receptor in a linear fashion, with the ligand amine interacting with E172 and the longer of two hydrophobic substituents binding in the primary hydrophobic region adjacent to the α4 and α5 helices. This binding mode was reproduced in the top-ranked docked solutions for the co-crystallized ligands, which also occupied the top positions in the rank-ordered list of poses based on the total GlideScore (Figure S1A and S1E; Table S3, Column A,

Supplementary Information). The conformations of the four antagonist-bound receptor crystal structures are very similar,[14] and the three non-PD144418 antagonists not only fit into the binding site, but actually docked to the PD144418-antagonized structure with a better (i.e. lower) GlideScore than did PD144418 itself (Table S4). The best-scoring docking pose for the reference antagonist PB212 matched previously-published results, with the naphthyl moiety engaging in aromatic interactions with Y103 and other hydrophobic residues in the primary hydrophobic region and the methoxy group interacting with Y206 on the α5 helix, and the 4-methylpiperidine moiety bound in the secondary hydrophobic site (Figure S1B).[41] Interestingly, docked solutions for the agonist (+)-pentazocine were also identified in the antagonized receptor, but (perhaps expectedly) with poorer scores than those in the (+)-pentazocine-agonized structure (Figure S1F and Table S3; Figure 3 and Table S4). It is conceivable that the poses in the PD144418-antagonized receptor represent alternative and/or intermediate binding modes that lead to the one(s) resulting in maximal agonism of the receptor. Similarly, linear binding modes for agonists **1a** and **1b** were also identified in the PD144418-antagonized receptor in which the *p*-chlorophenoxy or *p*-methoxyphenoxy moiety interacts with Y103 and other hydrophobic residues in the primary hydrophobic region (Figure S1C and S1D).

Interactions of the docked antagonists with the (+)-pentazocine-agonized conformation of the receptor were qualitatively like those found in the PD144418-antagonized conformation, although the docking scores were generally poorer due to less efficient hydrophobic packing of the bulky hydrophobic side chains with the ligand in the more spacious agonist binding site conformation (Figure 3B, 3E, 3F and Table S4). (+)-Pentazocine specifically stabilizes a conformation of the receptor in which the α4 helix is shifted approximately 1.8 Å away from the α5 helix *via* direct steric and H-bond interaction with A185 (Figure 3A).[14] Unlike for the docked antagonists, binding modes for the agonists **1a** and **1b** were identified that exhibit a more direct interaction with the α4 helix in its "outward" conformation. For compound **1a**, a halogen bond between the *p*-chloro group of the ligand and the T181 backbone oxygen atom of the receptor stabilizes the outward position of the α4

helix (Figure 3C). For compound **1b**, the ligand adopts a more nearly linear conformation but the *p*-methoxy group interacts specifically with the T181 side chain (Figure 3D). To avoid unfavorable nonpolar–polar interactions of the ligand methoxy $-CH_3$ group with the receptor T181 side chain –OH group, the T181 χ_1 bond angle must rotate from the *g*+ (*gauche*+) conformation to the *t* (*trans*) conformation, breaking the intramolecular H-bond with the I178 (*i*–3) backbone oxygen atom, weakening the rigidity of the α-helical backbone of α4, facilitating the movement of α4 away from α5 (Figure 3D). This is likely a more subtle effect than the helix-blocking halogen bond of **1a** and could explain the relatively lower potency of **1b** compared to **1a**.

Addition of a methyl group at the R_1 position (Table 1) introduces a degree of branching in the linker and a chiral center ((*R*)-**2a**, (*S*)-**2a**, (*R*)-**2b**, (*S*)-**2b**) while maintaining the high affinity of the parent compounds **1a** and **1b**. Our modeling results show that the R_1 position is located in a sterically tolerant region of the binding site and that the methylated analogs bind in a fashion qualitatively similar to the parent compounds **1a** and **1b**. Increasing the methyl substitution on the piperidine ring adjacent to the amine to *cis*-2,6-di-CH_3 (**5a** and **5b**) decreases, but does not abolish, compound affinity. In the docked solutions, the *cis*-2,6-di-CH_3 groups experience modest steric clashes with the receptor residue side chains in the vicinity of E172, causing the ligand to (in some cases) adopt "reverse" binding modes in which the *p*-chlorophenoxy or *p*-methoxyphenoxy substituent is bound in the secondary hydrophobic binding region rather than the larger primary hydrophobic binding region. Subsequently increasing the chain length of the linker by one methylene unit (**4a** and **4b**) *increases* the σ_1 affinity by allowing the chlorophenoxy or methoxyphenoxy moiety to fill the hydrophobic region in which it is situated more effectively and thus take advantage of additional hydrophobic interactions. Further increasing the degree of methylation to the 2,2,6,6-tetra-CH_3 (**6a** and **6b**) resulted in compounds with no measurable σ_1 affinity. Docked solutions for these compounds were either not found or characterized by several receptor–ligand bad contacts (steric clashes).

CONCLUSIONS

Based on the previously-identified lead compound 1-[ω-(4-chlorophenoxy)ethyl]-4-methylpiperidine (**1a**) and its methoxy-containing analog 1-[ω-(4-methoxyphenoxy)ethyl]-4-methylpiperidine (**1b**) reminiscent of the high-affinity ligand PB212 and its 6-methoxynaphthalen-1-yl moiety, a series of analogs was produced that featured varying degrees of methylation, particularly at carbon atoms *alpha* to the piperidine nitrogen atom. Several of these more sterically hindered analogs exhibited high σ_1 receptor affinity and selectivity, but 4-methylpiperidine was confirmed as optimal for σ_1 receptor affinity. Thus, steric hindrance around the nitrogen atom was confirmed to be detrimental for σ_1 receptor binding. In general, better binding profiles were obtained for the *p*-chloro-containing analogs compared to the *p*-methoxy-containing analogs. No difference in the functional activity conferred by the chloro *vs* methoxy group was observed—indeed, lead compounds **1a** and **1b** are both potent σ_1 receptor agonists, active *in vivo*. Molecular modeling techniques incorporating automated receptor–small-molecule ligand docking and ligand binding affinity data were employed to generate hypotheses about how the analogs bind to (or don't bind to) and activate (or don't activate) the σ_1 receptor. The interaction with T181 of the group in para-position on the phenoxy system appears to greatly contribute to the σ_1 receptor agonist functional activity. Finally, compound **1a** emerged for its strikingly potent σ_1 receptor-mediated antiamnesic properties and deserves further investigation in models of other σ_1-related pathologies in which σ_1 agonism would provide therapeutic benefit, also taking into consideration that it largely exceeds the σ_1 receptor affinity of ligands currently in clinical trials in several neurodegenerative diseases.

EXPERIMENTAL SECTION

Chemical Methods.

Synthesis. Column chromatography was performed on ICN silica gel 60Å (63–200 μm) as the stationary phase. Melting points were determined in open capillaries on a Gallenkamp electrothermal apparatus and are uncorrected. Mass spectra were recorded with a HP GC/MS 6890-5973 MSD spectrometer, electron impact 70 eV, equipped with HP ChemStation. ^{1}H NMR spectra

were recorded in $CDCl_3$ or CD_3OD on a Bruker AM 300 WB (300 MHz) spectrometer. For optical isomers, NMR spectra are identical and reported only for one of the two enantiomers. Chemical shifts are expressed as parts per million (δ). ^{13}C NMR (125 MHz) were recorded in $CDCl_3$ on a 500-vnmrs500 agilent spectrometer (499,801 MHz) for in vivo tested compounds (**1a**,**b**) . Analytical HPLC were performed on an Agilent 1260 Infinity Binary LC System equipped with a diode array detector using a revesed phase column (Phenomenex Gemini C-18, 5 μm, 250 × 4.6 mm). Microanalyses of solid compounds were carried out with a Carlo Erba 1106 analyzer; the analytical results are within ±0.4% of the theoretical values. Optical rotations were measured with a Perkin-Elmer 341 polarimeter at room temperature (20°C): concentrations are expressed as g/100 mL. Chemicals were purchased from Aldrich and were used without any further purification.

Preparation of 4-Methyl-1-[2-(aryloxy)ethyl]piperidine Hydrochloride (1a,b). A solution of 4-methylpiperidine (1.12 g, 11.2 mmol) in dry THF (50 mL) was added with K_2CO_3 (1.54 g, 11.2 mmol). After 10 min, a solution of **7b** (2.5 g, 10.2 mmol) in dry THF (40 mL) was added, the mixture was refluxed with stirring for 10h and the solvent was removed under reduced pressure. The residue was dissolved in Et_2O, washed with water and extracted with 2 N HCl. The collected aqueous phases were alkalized with 6 N NaOH and extracted with Et_2O. The solvent was washed with brine, dried over Na_2SO_4 and evaporated *in vacuo* to afford the desired piperidine as yellow oil in 50% yield. The corresponding hydrochloride salts were prepared by adding a HCl saturated ethereal solution to an ethereal solution of the amine.

4-Methyl-1-[2-(4-chlorophenoxy)ethyl]piperidine Hydrochloride (1a): Yield, GC/MS and ^1H NMR in accordance to the previously reported procedure.[38] ^{13}C NMR (free amine) 21.8, 30.5, 34.3, 54.5, 57.2, 66.4, 125.7, 129.3, 133.7, 157.5. Hydrochloride salt was > 98 % pure by HPLC analysis performed by isocratic elution with $CH_3CN/HCOONH_4$ (20 mM, pH =5) 80:20 v/v, at a flow rate of 1 mL/min.

4-Methyl-1-[2-(4-methoxyphenoxy)ethyl]piperidine Hydrochloride (1b): Yield: 27%; GC/MS *m/z* (free amine) 249 (M^+, 2), 112 (100); ^{1}H NMR (CD_3OD): δ 1.02 (d, 3H, CH_3), 1.40–2.10 (m, 5H, CH_2CHCH_2, piperidine), 2.60–3.00 (m, 2H, 2 of piperidine CH_2NCH_2), 3.40 (t, 2H, OCH_2CH_2), 3.50–3.70 (m, 2H, 2 of piperidine CH_2NCH_2), 3.73 (s, 3H, CH_3O), 4.48 (t, 2H, OCH_2), 6.75–6.80 (m, 4H, aromatic), 12.52 (bs, 1H, NH^+, D_2O exchanged). ^{13}C NMR (free amine) 21.8, 30.5, 34.3, 54.5, 56.0, 57.2, 66.4, 114.6, 115.6, 153.0, 153.8. Hydrochloride salt was > 98 % pure by HPLC analysis performed by isocratic elution with $CH_3CN/HCOONH_4$ (20 mM, pH =5) 80:20 v/v, at a flow rate of 1 mL/min.

Preparation of (–)-(*S*)- and (+)-(*R*)-1-(4-Methoxyphenoxy)-2-(4-methyl-2,6-piperidindion-1-yl)propane. A solution of 3-methylglutaric acid (6.3 mmol) in acetyl chloride (6.6 mL) was stirred under reflux for 2h. After cooling, acetyl chloride excess was removed under reduced pressure. The oily residue was dissolved in dry THF (20 mL) and the solvent was distilled off under vacuum; this operation was repeated five times affording a light brown solid to which a solution of the appropriate amine **9** (6.3 mmol) in dry THF (10 mL) was added. The reaction mixture was stirred for 12h at room temperature, the solvent was evaporated under vacuum and acetyl chloride (5.5 mL) was added to the oily residue. After refluxing for 4h, the mixture was evaporated to dryness under reduced pressure affording a red-brown oil which was dissolved in CH_2Cl_2 (50 mL) and washed with Na_2CO_3 saturated solution, brine and 2 N HCl followed by brine. The organic layer was dried over Na_2SO_4 and filtered. The solvent was evaporated *in vacuo* to obtain an oily residue which was chromatographed on a silica gel column (petroleum ether/ethyl acetate 7:3 as eluent) affording (S) or (R) enantiomers as pale-yellow oils.

(–)-(*S*)-1-(4-Methoxyphenoxy)-2-(4-methyl-2,6-piperidindion-1-yl)propane: 60% yield; $[\alpha]_D$= –26 (*c* 1.3, MeOH); GC/MS *m/z* 291(M^+, 1), 168 (100); ^{1}H NMR ($CDCl_3$): δ 1.05 (d, 3H, piperidine CH_3), 1.38 (d, 3H, CH_3CHN), 2.05–2.80 (m, 5H, CH_2CHCH_2, piperidine), 3.74 (s, 3H, CH_3O), 4.00–4.50 (m, 2H, CH_2O), 5.10–5.30 (m, 1H, CHN), 6.70–6.80 (m, 4H, aromatic).

(+)-(*R*)-1-(4-Methoxyphenoxy)-2-(4-methyl-2,6-piperidindion-1-yl)propane: 70% yield; $[\alpha]_D$= +25 (*c* 1.3, MeOH).

Preparation of (–)-(*S*)- or (+)-(*R*)-1-[2-(4-Methoxyphenoxy)-1-methyl-ethyl]-4-methyl-piperidine Hydrochlorides [(*S*)-2b, (*R*)-2b]. A solution of BMS (18.5 mmol) in anhydrous THF (10 mL) was carefully added dropwise to a stirred and ice-bath cooled solution of the appropriate piperidindion (3.7 mmol) in anhydrous THF (20 mL). The reaction mixture was refluxed with stirring for 2h, cooled to 0°C and carefully added with MeOH (20 mL) to destroy the excess of boran complex. Then, 2 N HCl (40 mL) was added and the resulting mixture was refluxed with stirring for 2h. After distilling off the organic solvents, the mixture was allowed to cool at room temperature and alkalized with 6 N NaOH. The aqueous layer was extracted with ethyl acetate (3×50 mL) and the combined organic extracts were washed with brine (1×40 mL), dried over Na_2SO_4 and filtered. Evaporation of the solvent *in vacuo* afforded the desired piperidines as pale-yellow oils in quantitative yields. The corresponding hydrochloride salts were prepared according to the procedure reported above for compounds **1b**. Recrystallization solvent, crystallization formula, $[\alpha]_D$ and melting point are listed in Table 1. Both the title compounds were obtained as white crystalline powders.

(–)-(*S*)-1-[2-(4-Methoxyphenoxy)-1-methyl-ethyl]-4-methyl-piperidine hydrochloride [(*S*)-2b]: 68% yield; GC/MS *m/z* (free amine) 263 (M^+, 1), 126 (100); ^{1}H NMR (CD_3OD): δ 1.02 (d, 3H, piperidine CH_3), 1.57 (d, 3H, C*H*$_3$CH), 1.70–2.20 (m, 5H, CH_2CHCH_2, piperidine), 2.80–3.10 (m, 2H, 2 of piperidine CH_2NCH_2), 3.40–3.70 (m, 3H, 2 of piperidine CH_2NCH_2 and CHN), 3.78 (s, 3H, OCH_3), 4.10–4.50 (m, 2H, OCH_2), 6.80–6.93 (m, 4H, aromatic), 12.11 (bs, 1H, NH^+, D_2O exchanged).

(+)-(*R*)-1-[2-(4-Methoxyphenoxy)-1-methyl-ethyl]-4-methyl-piperidine hydrochloride [(*R*)-2b]: 43% yield.

Preparation of (*R*)- or (*S*)-1-(Aryloxyethyl)-2-methylpiperidine Hydrochlorides (3a,b). General procedure. (*R*)-2-methylpiperidine, prepared following a procedure described in

literature,[46] (or commercially available (*S*) enantiomer) was added to a solution of NaOH (15.0 mmol) in water (20 mL) and 2-propanol (15 mL). The resulting mixture was cooled to 0°C with stirring for 10 min, then a solution of **7a** (or **7b**) (14.0 mmol) in 2-propanol (100 mL) was added dropwise. The reaction mixture was stirred at 0°C for 30 min and refluxed for 7h; the organic solvent was removed under reduced pressure and the aqueous phase was acidified with 6 N HCl, washed with Et_2O, alkalized with 6 N NaOH and extracted with Et_2O. The organic layer was washed with brine, dried over Na_2SO_4 and filtered; the solvent was evaporated *in vacuo* to afford the desired piperidines as pale yellow oils in 20–40% yields. The corresponding hydrochloride salts were prepared according to the procedure reported above for compounds **1b**. Recrystallization solvent, crystallization formula, $[\alpha]_D$ and melting point are listed in Table 1. All of the title compounds were obtained as white crystalline powders.

(–)-(*R*)-2-Methyl-1-[2-(4-chlorophenoxy)ethyl]piperidine hydrochloride [(*R*)-3a]: 25% yield; GC/MS *m/z* (free amine) 253 (M^+, 1), 112 (100); ^{1}H NMR (CD_3OD): δ 1.15–2.20 (m, 9H, CH_3 and $3CH_2$, piperidine), 3.00–3.80 (m, 5H, OCH_2CH_2, CH and NCH_2 of piperidine), 4.00–4.75 (m, 2H, OCH_2), 6.80–7.40 (m, 4H, aromatic), 12.50 (bs, 1H, NH^+, D_2O exchanged).

(+)-(*S*)-2-Methyl-1-[2-(4-chlorophenoxy)ethyl]piperidine hydrochloride [(*S*)-3a]: 32% yield.

(–)-(*R*)-2-Methyl-1-[2-(4-methoxyphenoxy)ethyl]piperidine hydrochloride [(*R*)-3b]: 21% yield; GC/MS *m/z* (free amine) 249 (M^+**,** 4), 112 (100); ^{1}H NMR (CD_3OD): δ 1.10–2.50 (m, 9H, CH_3 and $3CH_2$, piperidine), 2.70–3.70 (m, 5H, OCH_2CH_2, CH and NCH_2 of piperidine), 3.80 (s, 3H, OCH_3), 4.10–4.60 (m, 2H, OCH_2), 6.80–7.00 (m, 4H, aromatic), 12.55 (bs, 1H, NH^+, D_2O exchanged).

(+)-(*S*)-2-Methyl-1-[2-(4-methoxyphenoxy)ethyl]piperidine hydrochloride [(*S*)-3b]: 23% yield.

Preparation of *cis*-1-(3-Aryloxypropyl)-2,6-dimethylpiperidine Salts (4a, 4b). General procedure. To a solution of **8a** (or **8b**) (7.1 mmol) in dry toluene (12 mL) were added *cis*-2,6-

dimethylpiperidine (7.8 mmol) and 1,2,2,6,6-pentamethylpiperidine (7.8 mmol).[47] The resulting mixture was refluxed with stirring for 24h and then was allow to cool to room temperature. The solid was filtered off and the filtrate was concentrated *in vacuo*, diluted with ethyl acetate and extracted with 6 N HCl. The collected aqueous extracts were washed with Et_2O, alkalized with 6 N NaOH and extracted with $CHCl_3$. The organic layer was washed with brine and dried over Na_2SO_4; the solvent was removed under reduced pressure to afford the desired piperidines as pale yellow oils in 40–65% yields. The hydrochloride salt **4a** was prepared according to the procedure reported above for compounds **1b**. The oxalate salt **4b** was prepared by adding an equimolar amount of oxalic acid to a solution of the piperidine in abs. EtOH. Recrystallization solvent, crystallization formula, $[\alpha]_D$ and melting point are listed in Table 1. All of the title compounds were obtained as white crystalline powders.

***cis*-1-[3-(4-Chlorophenoxy)propyl]-2,6-dimethylpiperidine hydrochloride (4a):** 32% yield; GC/MS *m/z* (free amine) 283 (M^++2, 2), 281 (M^+, 6), 266 (100); ^{1}H NMR (CD_3OD): δ 1.40–1.60 (m, 6H, $2CH_3$), 1.60–2.20 (m, 6H, $3CH_2$, piperidine), 2.20–2.50 (m, 2H, OCH_2CH_2), 2.90–3.10 (m, 2H, 2CH), 3.40–3.55 (t, 2H, CH_2N), 3.95–4.15 (m, 2H, CH_2O), 6.70–7.30 (m, 4H, aromatic), 11.50–11.90 (bs, 1H, NH^+, D_2O exchanged).

***cis*-1-[3-(4-Methoxyphenoxy)propyl]-2,6-dimethylpiperidine oxalate (4b):** 42% yield; GC/MS *m/z* (free amine) 277 (M^+, 9), 262 (100); ^{1}H NMR (CD_3OD): δ 1.20–1.50 (m, 6H, $2CH_3$), 1.60–2.30 (m, 8H, $3CH_2$ of piperidine and OCH_2CH_2), 2.80–3.20 (m, 2H, 2CH), 3.40–3.60 (t, 2H, CH_2N), 3.74 (s, 3H, OCH_3), 3.97 (t, 2H, CH_2O), 6.70–6.90 (m, 4H, aromatic), 9.20–10.40 (bs, 1H, NH^+, D_2O exchanged).

Preparation of *cis*-1-[(Aryloxy)acetyl]-2,6-dimethylpiperidines. General procedure. To a stirred solution of **10b** (or commercially available **10a**) (5.0 mmol) in anhydrous CH_2Cl_2 (25 mL), *N*,*N*'-dicyclohexylcarbodiimide (DCC, 5.2 mmol) and *cis*-2,6-dimethylpiperidine (5.2 mmol) were added. The resulting mixture was stirred for 24h at room temperature and diluted with CH_2Cl_2 (80 mL). The precipitate was filtered off and the solution was washed with 2 N HCl (2×75 mL), followed

by brine (1×75 mL), $NaHCO_3$ saturated solution (2×75 mL) and brine (1×75 mL); then it was dried over Na_2SO_4 and filtered. The solvent was evaporated *in vacuo* to afford a white solid which was chromatographed on silica gel column (petroleum ether/ethyl acetate 6:4 as eluent). The desired compounds were obtained as pale-yellow oils in 25–44% yields.

***cis*-1-[(4-Chlorophenoxy)acetyl]-2,6-dimethylpiperidine:** 25% yield; GC/MS *m/z* 283 (M^++2, 15), 281 (M^+, 43), 140 (100).

***cis*-1-[(4-Methoxyphenoxy)acetyl]-2,6-dimethylpiperidine:** 44% yield; GC/MS *m/z* 277 (M^+, 100); ^{1}H NMR ($CDCl_3$): δ 1.28–1.90 (m, 12H, $2CH_3$ and $3CH_2$, piperidine), 3.75 (s, 3H, OCH_3), 4.14–4.63 (m, 4H, OCH_2 and 2CH), 6.80–6.90 (m, 4H, aromatic).

Preparation of *cis*-1-[(Aryloxy)acetyl]-2,2,6,6-tetramethylpiperidines. General procedure. Thionyl chloride (107.0 mmol) was added to **10a** (or **10b**) (10.7 mmol) and the mixture was refluxed with stirring for 1h. After distilling off the thionyl chloride excess, the oily residue was dissolved in dry CH_2Cl_2 (50 mL) and added to a stirred solution of Et_3N (12.7 mmol) and 2,2,6,6-tetramethylpiperidine (11.6 mmol) in dry CH_2Cl_2 (40 mL), under N_2 atmosphere. The mixture was stirred for 3h at room temperature. The organic layer was washed with $NaHCO_3$ saturated solution, followed by brine, 3 N HCl and brine; then it was dried over Na_2SO_4 and filtered. The solvent was removed under reduced pressure affording a white solid which was chromatographed on silica gel column (petroleum ether/ethyl acetate 9:1 as eluent). The desired compounds were obtained as pale-yellow oils in 55–58% yields.

1-[(4-Chlorophenoxy)acetyl]-2,2,6,6-tetramethylpiperidine: 58% yield; GC/MS *m/z* 309 (M^+, 4), 294 (100); ^{1}H NMR ($CDCl_3$): δ 1.48 (s, 12H, $4CH_3$), 1.76 (s, 6H, $3CH_2$), 4.60 (s, 2H, OCH_2), 6.83–7.24 (m, 4H, aromatic).

1-[(4-Methoxyphenoxy)acetyl]-2,2,6,6-tetramethylpiperidine: 55% yield; GC/MS *m/z* 305 (M^+, 49), 69 (100); ^{1}H NMR ($CDCl_3$): δ 1.48 (s, 12H, $4CH_3$), 1.75 (s, 6H, $3CH_2$), 3.75 (s, 3H, OCH_3), 4.58 (s, 2H, OCH_2), 6.80–6.88 (m, 4H, aromatic).

Preparation of Aryloxyethylpiperidine Hydrochlorides 5a,b and **6a,b. General procedure.** A solution of boran–methyl sulfide complex (BMS, 12.0 mmol) in anhydrous THF (3 mL) was carefully added dropwise to a stirred and cooled to 0°C solution of the appropriate amide (3 mmol) in anhydrous THF (15 mL). The reaction mixture was refluxed with stirring for 4h, cooled to 0°C and carefully added with methanol (15 mL) to destroy the boran complex excess. Then, 6 N HCl (15 mL) was added and the resulting mixture was refluxed with stirring for 1h. After distilling off the organic solvents, the mixture was allowed to cool at room temperature and alkalized with 6 N NaOH. The aqueous solution was extracted with $CHCl_3$ (3×40 mL) and the combined organic extracts were washed with brine (1×40 mL), dried over Na_2SO_4 and filtered. Evaporation of the solvent *in vacuo* afforded the desired piperidines as pale-yellow oils in quantitative yields. The corresponding hydrochloride salts were prepared by adding a HCl saturated ethereal solution to an ethereal solution of the amine. Recrystallization solvent, $[\alpha]_D$, crystallization formula and melting point are listed in Table 1. All of the title compounds were obtained as white crystalline powders.

***cis*-1-[2-(4-Chlorophenoxy)ethyl]-2,6-dimethylpiperidine hydrochloride (5a):** 82% yield; GC/MS *m/z* (free amine) 267 (M^+, 1), 126 (100); ^{1}H NMR (CD_3OD): δ 1.20–2.35 (m, 12H, $2CH_3$ and $3CH_2$, piperidine), 3.23–3.65 (m, 2H, 2CH), 3.72 (t, 2H, CH_2N), 4.30 (t, 2H, OCH_2), 6.81–7.28 (m, 4H, aromatic), 12.04 (bs, 1H, NH^+, D_2O exchanged).

***cis*-1-[2-(4-Methoxyphenoxy)ethyl]-2,6-dimethylpiperidine hydrochloride (5b):** 35% yield; GC/MS *m/z* (free amine) 263 (M^+, 3), 126 (100); ^{1}H NMR (CD_3OD): δ 1.51–2.39 (m, 12H, $2CH_3$ and $3CH_2$, piperidine), 3.30–3.62 (m, 2H, 2CH), 3.70 (bs, 2H, CH_2N), 3.75 (s, 3H, OCH_3), 4.26 (bs, 2H, OCH_2), 6.82 (m, 4H, aromatic), 11.90 (bs, 1H, NH^+, D_2O exchanged).

1-[2-(4-Chlorophenoxy)ethyl]-2,2,6,6-tetramethylpiperidine hydrochloride (6a): 70% yield; GC/MS *m/z* (free amine) 295 (M^+, 1), 154 (100); ^{1}H NMR (CD_3OD): δ 1.35 (s, 6H, $2CH_3$, piperidine), 1.56–1.98 (m, 10H, $2CH_3$ + $CH_2C\mathit{H}_2CH_2$ + 2 of $C\mathit{H}_2CH_2C\mathit{H}_2$, piperidine), 2.55–2.75 (m, 2H, 2 of $C\mathit{H}_2CH_2C\mathit{H}_2$, piperidine), 3.20–3.40 (m, 2H, CH_2N), 4.59 (t, 2H, OCH_2), 6.84–7.20 (m, 4H, aromatic), 10.76 (bs, 1H, NH^+, D_2O exchanged).

1-[2-(4-Methoxyphenoxy)ethyl]-2,2,6,6-tetramethylpiperidine hydrochloride (6b): 24% yield; GC/MS *m/z* (free amine) 291 (M^+, 2), 154 (100); ^{1}H NMR (CD_3OD): δ 1.35 (s, 6H, $2CH_3$, piperidine), 1.57–1.94 (m, 10H, $2CH_3$ + $CH_2CH_2CH_2$ + 2 of $CH_2CH_2CH_2$, piperidine), 2.62–2.68 (m, 2H, 2 of $CH_2CH_2CH_2$, piperidine), 3.20–3.40 (m, 2H, CH_2N), 3.73 (s, 3H, OCH_3), 4.58 (t, 2H, OCH_2), 6.74–6.90 (m, 4H, aromatic), 10.71 (bs, 1H, NH^+, D_2O exchanged).

Preparation of Aryloxyalkyl Alcohols. General procedure. 2-Chloroethanol (or 3-chloropropanol) (12.0 mmol) was added to a stirred and warmed up to 40°C solution of the appropriate 4-substitued phenol (15.0 mmol) in 10% NaOH (10 mL). The resulting mixture was refluxed with stirring for 2–3h and then was allowed to cool to room temperature and extracted with Et_2O (3×20 mL). The combined organic extracts were washed with 10% NaOH (2×10 mL) followed by brine (2×10 mL) and then dried over Na_2SO_4 and filtered. The solvent was evaporated *in vacuo* to afford the desired products as colorless oils in 54–81% yields.

2-(4-Chlorophenoxy)ethanol: 68% yield; GC/MS *m/z* 174 (M^++2, 13), 172 (M^+, 37), 128 (100);

^{1}H NMR ($CDCl_3$): δ 2.10 (bs, 1H, OH, D_2O exchanged), 3.95 (t, 2H, CH_2OH), 4.10 (t, 2H, $ArOCH_2$), 6.70–7.20 (m, 4H, aromatic).

2-(4-Methoxyphenoxy)ethanol: 81% yield; GC/MS *m/z* 168 (M^+, 57), 124 (100); ^{1}H NMR ($CDCl_3$): δ 2.35 (s, 1H, OH, D_2O exchanged), 3.80 (s, 3H, OCH_3), 3.85–4.50 (m, 4H, OCH_2CH_2), 6.70–7.00 (m, 4H, aromatic).

3-(4-Chlorophenoxy)-1-propanol: 54% yield; GC/MS *m/z* 188 (M^+ +2, 11), 186 (M^+, 32), 128 (100);

^{1}H NMR ($CDCl_3$): δ 1.85–2.20 (m, 3H, $CH_2CH_2CH_2$ and OH, D_2O exchanged), 3.85 (t, 2H, CH_2OH), 4.10 (t, 2H, $ArOCH_2$), 6.70–7.40 (m, 4H, aromatic).

3-(4-Methoxyphenoxy)-1-propanol: 62% yield; GC/MS *m/z* 182 (M^+, 54), 124 (100); ^{1}H NMR ($CDCl_3$): δ 1.79 (bs, 1H, OH, D_2O exchanged), 2.02 (m, 2H, $CH_2CH_2CH_2$), 3.76 (s, 3H, OCH_3), 3.86 (t, 2H, CH_2OH), 4.08 (t, 2H, $ArOCH_2$), 6.70–6.90 (m, 4H, aromatic).

Preparation of Aryloxyethylsulfonates 7a,b. General procedure. A solution of methanesulfonyl chloride (34.2 mmol) in anhydrous CH_2Cl_2 (20 mL) was added dropwise to a stirred and ice-bath cooled solution of the opportune 2-aryloxyethanol (13.7 mmol) and Et_3N (25.0 mmol) in anhydrous CH_2Cl_2 (40 mL). The reaction mixture was stirred at 0°C for 4h and then carefully poured into ice–water. The organic layer was separated and washed with cold 2 N HCl (2×20 mL) followed by brine (2×20 mL), $NaHCO_3$ saturated solution (2×20 mL) and brine (2×20 mL). Then, it was dried over Na_2SO_4 and filtered. The solvent was evaporated *in vacuo* to afford the desired products as pale yellow oils which were used for the next step without any further purification.

O-Methanesulfonyl-2-(4-Chlorophenoxy)ethanol (7a): 85% yield; GC/MS *m/z* 252 (M^++2, 12), 250 (M^+, 30), 123 (100); ^{1}H NMR ($CDCl_3$): δ 3.13 (s, 3H, SCH_3), 4.19–4.21 (m, 2H, $PhOCH_2$), 4.50–4.60 (m, 2H, CH_2OSO_2), 6.80–7.30 (s, 4H, aromatic).

O-Methanesulfonyl-2-(4-Methoxyphenoxy)ethanol (7b): 81% yield; GC/MS *m/z* 246 (M^+, 48), 123 (100); ^{1}H NMR ($CDCl_3$): δ 3.20 (s, 3H, SCH_3), 3.80 (s, 3H, OCH_3), 4.20–4.40 (m, 2H, $PhOCH_2$), 4.50–4.60 (m, 2H, CH_2OSO_2), 6.80–7.00 (m, 4H, aromatic).

Preparation of Aryloxypropylsulfonates (8a,b). General procedure. To a stirred solution of the opportune 3-aryloxypropanol (15.6 mmol) and Et_3N (31.2 mmol) in anhydrous CH_2Cl_2 (25 mL) was added dropwise a solution of 4-toluene-sulphonyl chloride (23.4 mmol) in anhydrous CH_2Cl_2 (20 mL). The resulting mixture was stirred at room temperature for 3h and the organic phase was washed with water, 2 N HCl (2×20 mL), $NaHCO_3$ saturated solution (2×20 mL) followed by brine (2×20 mL); then the organic layer was dried over Na_2SO_4 and filtered. The solvent was removed under reduced pressure affording a white solid which was chromatographed on silica gel column (petroleum ether/ethyl acetate 85:15 as eluent). Compounds **8a,b** were obtained as white solids in 40–45% yield.

O-(4-Methylbenzene)sulfonyl-3-(4-chlorophenoxy)-1-propanol (8a): 45% yield; GC/MS *m/z* 342 (M^++2, 10), 340 (M^+, 26), 155 (100).

O-(4-Methylbenzene)sulfonyl-3-(4-methoxyphenoxy)-1-propanol (8b): 40% yield; GC/MS *m/z* 336 (M^+, 62), 155 (100); ^{1}H NMR ($CDCl_3$): δ 2.09 (m, 2H, $CH_2CH_2CH_2$), 2.39 (s, 3H, CH_3), 3.77 (s, 3H, OCH_3), 3.89 (t, 2H, CH_2OPh), 4.23 (t, 2H, CH_2OSO_2), 6.60–7.80 (m, 8H, aromatic).

(–)-(*R*)- or (+)-(*S*)-2-Phthalimido-1-propanol. These compounds were prepared according to the published procedure and spectroscopic properties were identical to the data reported in literature.[38]

Preparation of (–)-(*S*)- or (+)-(*R*)-1-(4-Methoxyphenoxy)-2-phthalimidopropane. To a stirred solution of 4-methoxyphenol (30.0 mmol) and triphenylphosphine (30.0 mmol) in anhydrous THF (60 mL) was added the appropriate phthalimido alcohol (20.0 mmol) in anhydrous THF (30 mL). After cooling at 0°C, a solution of diisopropyl azodicarboxylate (DIAD, 30.0 mmol) in anhydrous THF (30 mL) was added dropwise and the reaction mixture was stirred overnight at room temperature, under N_2 atmosphere. The solvent was removed under reduced pressure and the residue was chromatographed on a silica gel column (petroleum ether/ethyl acetate 8:2 as eluent) affording (*S*)- or (*R*)-enantiomers as pale-yellow oils.

(–)-(*S*)-1-(4-Methoxyphenoxy)-2-phthalimidopropane: 75% yield; $[\alpha]_D$= –11 (*c* 1.5, MeOH); GC/MS *m/z* 311 (M^+, 21), 188 (100); ^{1}H NMR ($CDCl_3$): δ 1.53 (d, 3H, CH_3), 3.80 (s, 3H, OCH_3), 4.10–4.60 (m, 2H, CH_2O), 4.65–4.80 (m, 1H, CH), 6.70–6.90 (m, 4H, aromatic), 7.62–7.83 (m, 4H, aromatic).

(+)-(*R*)-1-(4-Methoxyphenoxy)-2-phthalimidopropane: 77% yield; $[\alpha]_D$= +12 (*c* 1.5, MeOH)

Preparation of (*S*)- or (*R*)-2-Amino-1-(4-methoxyphenoxy)propane (9). To a stirred solution of the appropriate aryloxyphthalimmidopropane (7.4 mmol) in MeOH (50 mL), glacial acetic acid (3 mL, 52.8 mmol) and hydrazine hydrate (55% solution, 3 mL, 51.5 mmol) were added. The reaction mixture was refluxed with stirring for 6h, then stirred overnight at room temperature. The solvent was removed under reduced pressure to afford a residue which was suspended in water. The aqueous phase was acidified with 6 N HCl, washed with Et_2O, alkalized with 6 N NaOH and extracted with $CHCl_3$. The organic layer was washed with brine, dried over Na_2SO_4 and filtered; then the

organic solvent was evaporated to dryness affording the expected amines as pale-yellow oils, which were used for the next step without any further purification.

(*S*)-2-Amino-1-(4-methoxyphenoxy)propane [(*S*)-9]: 70% yield; GC/MS *m/z* 181 (M^+, 17), 44 (100).

(*R*)-2-Amino-1-(4-methoxyphenoxy)propane [(*R*)-9]: 77% yield.

4-Methoxyphenoxyacetic acid (10b). A solution of 4-hydroxyanisole (2.71 g, 21.8 mmol) in abs. EtOH (30 mL) was added dropwise to an equimolar metallic sodium solution in abs. EtOH (30 mL). The resulting mixture was stirred for 10 min, added with a solution of ethyl bromoacetate (4 g, 24.0 mmol) in abs. EtOH (30 mL) and refluxed with stirring for 4h. The solvent was evaporated to dryness and the residue was dissolved in ethyl acetate. The organic layer was washed with 1 N NaOH and brine, dried over Na_2SO_4 and distilled off under reduced pressure affording a yellow oil (3.42 g, 16.3 mmol) which was dissolved in dry THF (100 mL) and 1 N NaOH (100 mL) and stirred at room temperature for 4 h. The organic layer was removed under reduced pressure and the aqueous phase was acidified with 6 N HCl and extracted with Et_2O. The organic layer was washed with brine dried over Na_2SO_4 and evaporated to dryness affording a white solid (2.09 g, 11.5 mmol) which was crystallized from hexane/$CHCl_3$. Yield: 58%; mp 109–11°C; ^{1}H NMR ($CDCl_3$): δ 3.77 (s, 3H, CH_3), 4.62 (s, 2H, CH_2), 4.70–4.90 (bs, 1H, COOH, D_2O exchanged), 6.70–6.90 (m, 4H, aromatic).

Biological Methods.

Radioligand Binding Assays. All the procedures for the binding assays were previously described. σ_1 and σ_2 receptor binding were carried out according to Matsumoto *et al.*[48] EBP binding was carried out according to Moebius *et al.*[49] [^{3}H]-**1** (30 Ci/mmol) and (+)-[^{3}H]-pentazocine (34 Ci/mmol) were purchased from PerkinElmer Life Sciences (Zavantem, Belgium). The radioligand (±)-[^{3}H]-emopamil (83 Ci/mmol) was purchased from American Radiolabeled Chemicals, Inc. (St. Louis, MO). Compound **1** and (±)-ifenprodil were purchased from Tocris Cookson Ltd., U.K. (+)-

Pentazocine and dizocilpine ((+)-MK-801 maleate) were obtained from Sigma-Aldrich-RBI (Milan, Italy; St Quentin-Fallavier, France).

Cell Cultures. SH-SY5Y neuroblastoma cells (CRL-2266™), human MCF7 adenocarcinoma cell lines (HTB-22™) and human HepG2 hepatocarcinoma cells (HB-8065™) were obtained from American Type Culture Collection (ATCC®, Bethesda, MD). SH-SY5Y cells were cultured in a 1:1 mixture of MEM and Ham's F12 Medium. This medium was supplemented with 10% (v/v) heat-inactivated Fetal Bovine Serum, 1% (v/v) Glutamine and 1% (v/v) Penicillin – Streptomycin. Cells were cultivated at 37 °C with 5% CO_2 at saturated humidity. MCF7 cells were cultured in DMEM supplemented with 10% (v/v) heat-inactivated Fetal Bovine Serum, 1% (v/v) Glutamine and 1% (v/v) Penicillin – Streptomycin, and incubated at 37 °C with 5% CO_2 at saturated humidity. HepG2 cells were cultured in MEM supplemented with 10% (v/v) heat-inactivated Fetal Bovine Serum, 1% (v/v) Glutamine and 1% (v/v) Penicillin – Streptomycin, 1% (v/v) NEAA, and incubated at 37 °C with 5% CO2 at saturated humidity.

Cell Viability. Determination of cell growth was performed using the MTT assay at 48 h.[50] On day 1, 25,000 cells/well were seeded into 96-well plates in a volume of 100 µL. On day 2, the various drug concentrations (1 µM-100 µM) were added. In all the experiments, the various drug-solvents (EtOH, DMSO) were added in each control to evaluate a possible solvent cytotoxicity. After the established incubation time with drugs (48 h), MTT (0.5 mg/mL) was added to each well, and after 3-4 h incubation at 37 °C, the supernatant was removed. The formazan crystals were solubilized using 100 µl of DMSO/EtOH (1:1) and the absorbance values at 570 and 630 nm were determined on the microplate reader Victor 3 from PerkinElmer Life Sciences.

In Vivo Assays. Male Dunkin guinea-pigs and Wistar Hannover rats (250–300 g) were from Harlan, Italy. Male Swiss OF-1 mice aged 7–9 weeks, were from Janvier (Le Genest-Saint-Isle, France). Mice were housed in the animal facility of the University of Montpellier (CECEMA), in groups of 8–10 mice, with free access to food and water, in a regulated environment (23 ± 1°C, 40–

60% humidity, 12 h light/dark cycle). Animal procedures were conducted in adherence with the European Union Directive 2010/63 and the ARRIVE guidelines[51] and authorized by the National Ethics Committee (Paris).

Drugs. 4-Methoxy-3-(2-phenylethoxy)-*N*,*N*-dipropyl-benzeneethanamine hydrochloride (NE-100) was purchased from Sigma-Aldrich (Saint-Quentin-Fallavier, France). Drugs were solubilized in physiological saline (NaCl 0.9%; vehicle solution) in a stock solution (1 mg/ml corresponding to a dose of 5 mg/kg) and dilutions done from this stock solution. The stock solutions were stored at +4°C for up to two weeks. Drugs were administered intraperitoneally (ip) in a volume of 100 µl per 20 g body weight.

Spontaneous alternation in the Y-maze. The Y-maze was made of grey polyvinylchloride. Each arm was 40 cm long, 13 cm high, 3 cm wide at the bottom, 10 cm wide at the top, and converging at an equal angle. Each mouse was placed at the end of one arm and allowed to move freely through the maze during an 8 min session. The series of arm entries, including possible returns into the same arm, were checked visually. An alternation is defined as entries into all three arms on consecutive occasions. The number of maximum alternations was therefore the total number of arm entries minus two and the percentage of alternation was calculated as (actual alternations / maximum alternations) × 100.[52-56] Exclusion criteria were: number of arm explored < 10 or percentage of alternation < 25% or > 90%. Animals showing these readouts were excluded from the calculations. Attrition is routinely < 5% in this test.

Step-through passive avoidance. The apparatus was a two-compartment (15 cm × 20 cm × 15 cm high) box with one compartment illuminated with white polyvinylchloride walls and the other darkened with black polyvinylchloride walls and a grid floor. A guillotine door separated the compartments. A 60-W lamp positioned 40 cm above the apparatus lit the white compartment during the experiment. Scrambled foot shocks (0.3 mA for 3 s) could be delivered to the grid floor using a shock generator scrambler (Lafayette Instruments, Lafayette, USA). The guillotine door was initially closed during the training session. Each mouse was placed into the white compartment. After 5 s, the

door was raised. When the mouse entered the darkened compartment and placed all its paws on the grid floor, the door is closed, and the foot shocks delivered for 3 s. The step-through latency, that is the latency spent to enter the darkened compartment, and the number of flinching reactions and/or vocalizations were recorded. The retention test was carried out 24 h after training. Each mouse was placed again into the white compartment. After 5 s, the door was raised. The step-through latency was recorded for up to 300 s.[53-56] Exclusion criteria were: latencies during training and retention < 10 s and no reaction to the shock. Animals showing these readouts were excluded from the calculations. Attrition is routinely < 5% in this test.

Computational Methods.

Molecular modeling. All modeling procedures were performed in Maestro 12.7 (Release 2021-1; Schrödinger, Inc., New York, NY). Default settings were employed unless otherwise noted. Modeled ligands included those that have been co-crystallized with the σ_1 receptor and structurally characterized (PD144418, 4-IBP, haloperidol, NE-100 and (+)-pentazocine), reference compounds PB190 and PB212 (Figure 1), and all other target compounds listed in Table 1, including the lead compounds **1a** and **1b**; these were sketched in their cationic (protonated) form and energy-minimized in the Maestro 3D Builder. The structures of the human σ_1 receptor bound to the high-affinity and selective antagonist PD144418 (PDB ID = 5HK1; 2.5 Å; chain 'A') and to the high-affinity and selective agonist (+)-pentazocine (PDB ID = 6DK1; 3.1 Å; chain 'A') were selected to represent antagonized and agonized conformational states of the receptor, respectively. The preprocessing, H-bond optimization, and restrained minimization (hydrogens only) steps were performed using the Protein Preparation wizard. Notably, the PROPKA H-bond optimization procedure neutralized (protonated) the D126 side chain. In its protonated form, D126 (along with Y103) thermodynamically and conformationally stabilizes the anionic E172 side chain within the ligand binding site. All ligands and water molecules in the crystal structure were removed prior to ligand docking. The ligand binding site was then defined and prepared using the Receptor Grid Generation wizard. The dimensions of the box enclosing the binding site were determined automatically using the co-crystallized ligands

(*i.e.*, PD144418 or (+)-pentazocine). An H-bond constraint was defined involving the oxygen atoms of the E172 side chain carboxylate group, which forms a salt-bridge interaction with the protonated ammonium ion of the ligand and that is observed in all experimentally-determined receptor–ligand complexes to date. Automated docking was then carried out with Prime and the Ligand Docking wizard within Maestro. Rigorous XP (extra precision) docking was performed, and the associated XP descriptor information was recorded. Sampling of conformers was enabled to model amine nitrogen inversions and alternative ring conformations. The initial (energy-minimized) input conformation of each ligand was also included. The E172 H-bond constraint previously defined during the grid generation step was enforced during the docking process. As many as 10 distinct poses (docked solutions) per ligand were retained. Using this methodology, the experimentally-observed docking poses of PD144418 and (+)-pentazocine were each reproduced as the highest-ranked solution for each ligand, providing validation for the docking method. The Pose Explorer and XP Visualizer tools within Maestro were used to analyze and visually interpret the resulting docked ligand poses, docking scores, and score components. Maestro was used also to prepare images of the σ_1 receptor–ligand complexes.

ASSOCIATED CONTENT

Elemental analyses of target compounds; Top-scoring poses for ligands in the PD144418-antagonized σ_1 site; Glide-XP scores and score components (PD144418-antagonized σ_1 site); Glide-XP scores and score components ((+)-pentazocine-agonized σ_1 site).

ACKNOWLEGMENTS

We thank the RAM-CECEMA animal facility of the University of Montpellier.

CONFLICT OF INTEREST

The authors declare no conflict of interest.

FIGURES and TABLES

Figure 1.

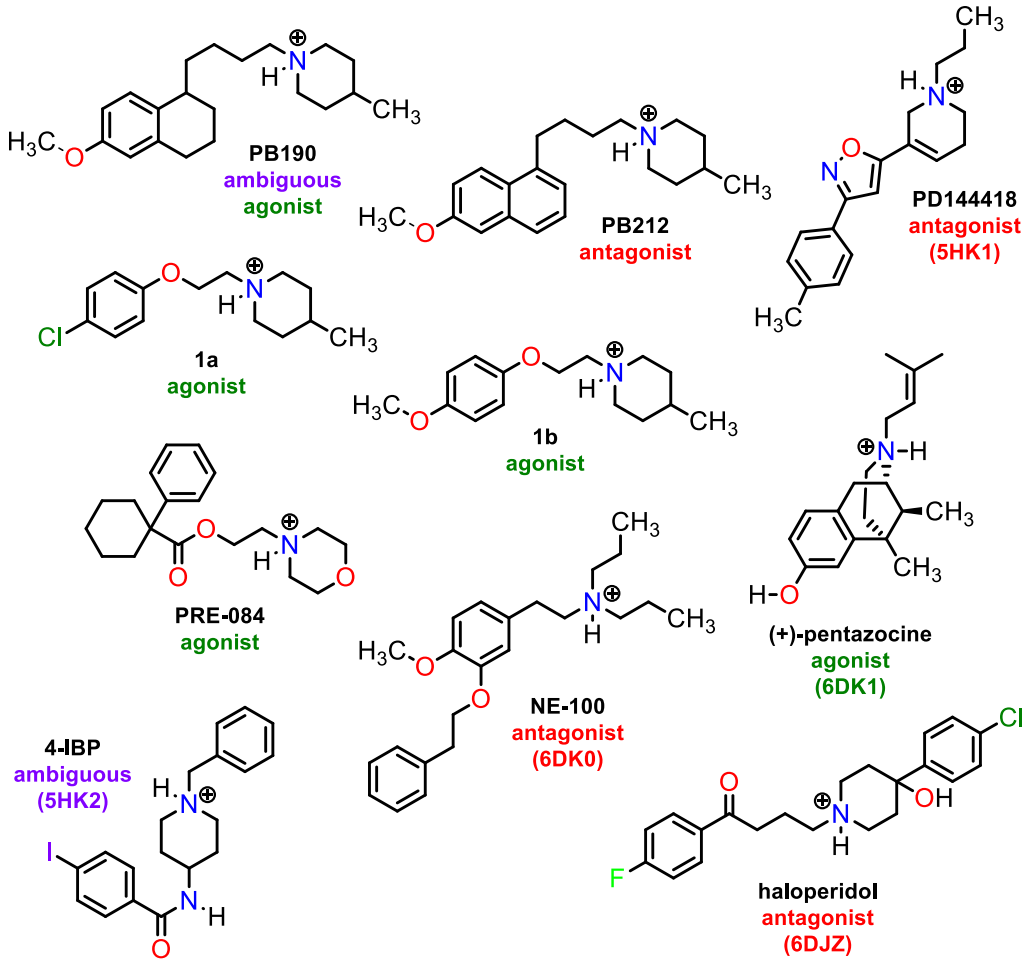

Figure 2.

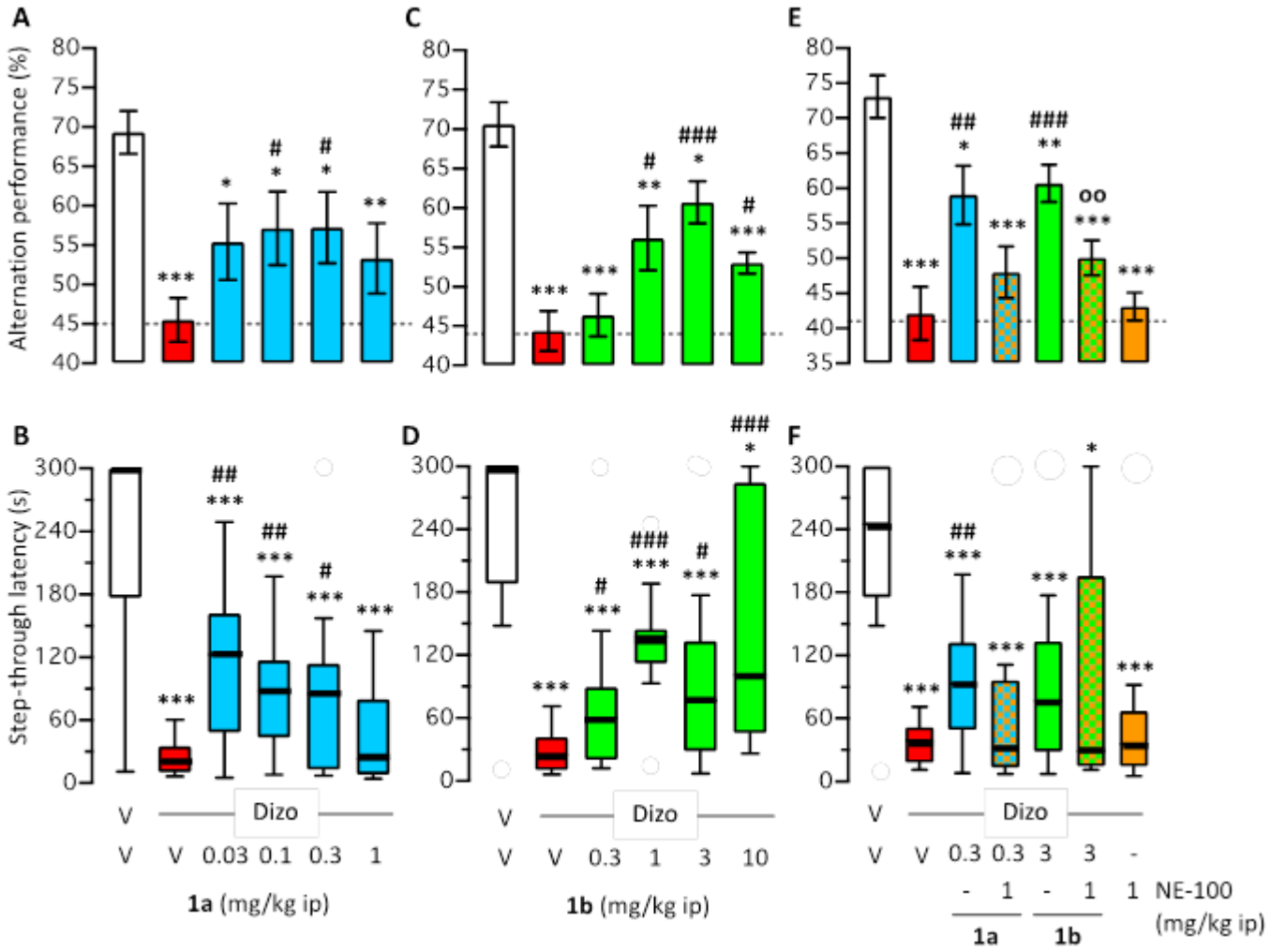
A
C
E
B
D
F
Alternation performance (%)
Step-through latency (s)
Dizo
V
0.03
0.1
0.3
1
3
10
1a (mg/kg ip)
1b (mg/kg ip)
NE-100 (mg/kg ip)
1a
1b

Figure 3.

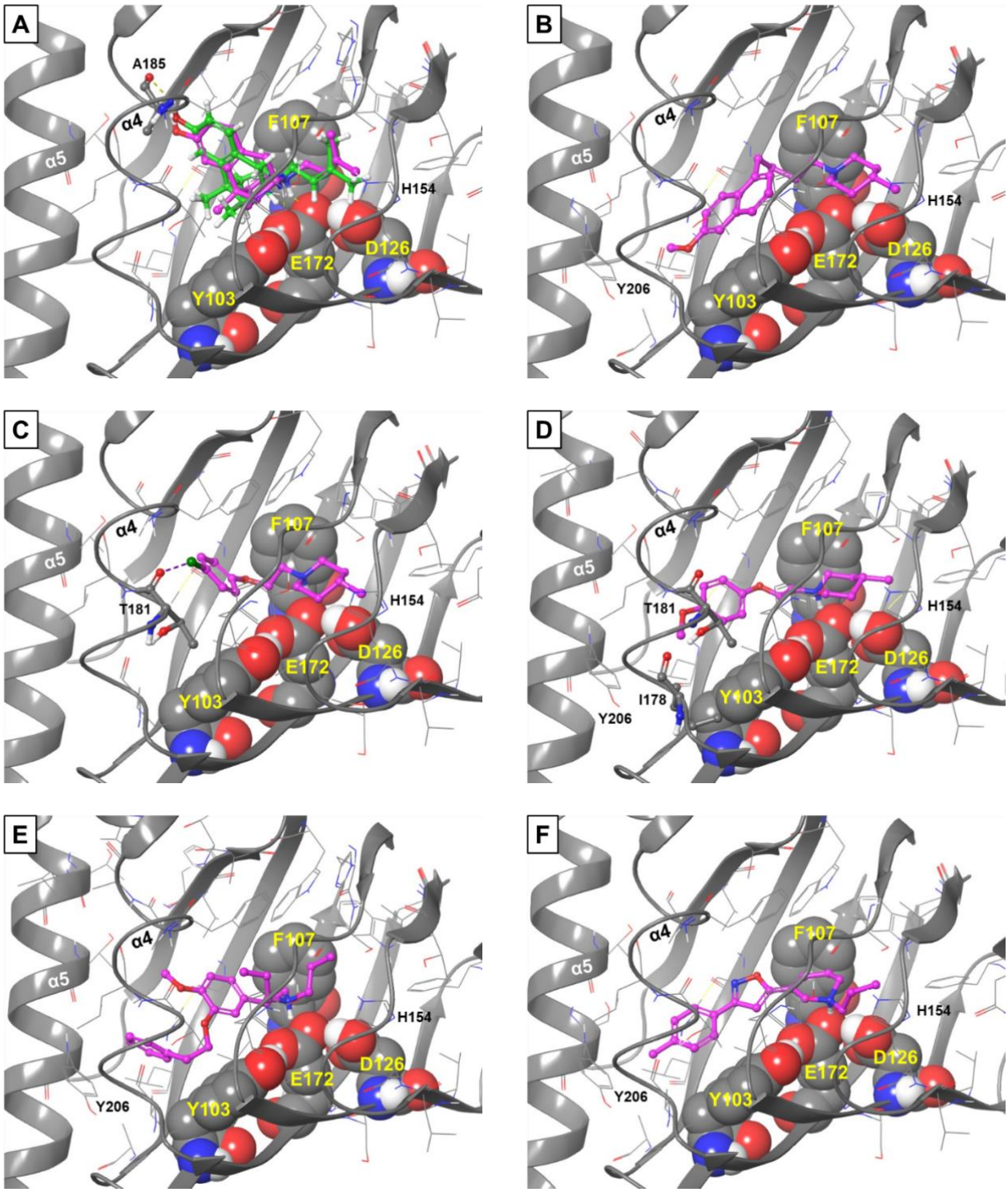
A
A185
α4
α5
F107
H154
E172
D126
Y103
B
α4
α5
F107
H154
E172
D126
Y206
Y103
C
α4
α5
F107
T181
H154
E172
D126
Y103
D
α4
α5
F107
T181
H154
E172
D126
I178
Y103
Y206
E
α4
α5
F107
H154
E172
D126
Y206
Y103
F
α4
α5
F107
H154
E172
D126
Y206
Y103

FIGURE CAPTIONS

Figure 1. Structures of reference and lead σ_1 receptor ligands in their protonated, σ_1 receptor-interacting form. Codes in parentheses are Protein Data Bank (PDB) IDs corresponding to the experimentally-determined σ_1 receptor structure in which the ligand is bound.

Figure 2. Effect of **1a** and **1b** on dizocilpine-induced learning deficits in mice: (A, C, E) alternation performance in the Y-maze and (B, D, F) step-through latency in the passive avoidance test. In (A-D), animals received **1a**, 0.03–1 mg/kg ip, or **1b**, 0.3–10 mg/kg ip, 10 min before dizocilpine (Dizo, 0.15 mg/kg ip), 20 min before the Y-maze test session or passive avoidance training. In (E, F), NE-100 (1 mg/kg ip) was administered simultaneously as **1a** or **1b** at the indicated dose. Retention in (B, D, F) was measured 24 h after training and is shown as median and interquartile range. One-way ANOVAs: $F_{(5,70)} = 4.10$, $p < 0.01$, n = 12–14 in (A); $F_{(5,78)} = 12.79$, $p < 0.0001$, n = 12–16 in (C); $F_{(6,80)} = 10.98$, $p < 0.0001$, n = 10–14 in (E). Kruskal–Wallis ANOVAs: $H = 35.25$, p < 0.0001, n = 12–14 in (B); $H = 39.51$, $p < 0.0001$, n = 12–16 in (D); $H = 24.68$, $p < 0.001$, n = 10–15 in (F). * $p < 0.05$, ** $p < 0.01$, *** $p < 0.001$ *vs*. (V+V)-treated group; # $p < 0.05$, ## $p < 0.01$, ### $p < 0.001$ *vs*. (V+Dizo)-treated group; oo $p < 0.01$, *vs*. (1b+Dizo)-treated group; Dunnett's test in (A, C, E), Dunn's test in (B, D, F).

Figure 3. Top-scoring docked poses for selected ligands in the (+)-pentazocine-***agonized*** σ_1 binding site (PDB ID = 6DK1). A) (+)-pentazocine. B) PB212. C) **1a**. D) **1b**. E) NE-100. F) PD144418. The ligands are displayed in ball-and-stick rendering with magenta-colored carbon atoms. The σ_1 receptor protein backbone is represented by a grey ribbon and its constituent amino acid residues in the vicinity of the docked ligand are displayed in either wire or CPK (space-filling) rendering with grey-colored carbon atoms. In panel A, the co-crystallized (+)-pentazocine ligand is displayed in ball-and-stick rendering with green-colored carbon atoms.

Table 1. Physical properties of target compounds.

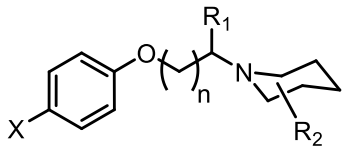

Compound	**X**	**n**	**R_1**	**R_2**	Formula[a]	mp (°C)	recrys. solv.[b]	$[\alpha]_D$[c]
1a[d]	Cl	1	H	4-CH_3	$C_{14}H_{20}ClNO{\cdot}HCl$	190–192	C	
(*R*)-**2a**[d]	Cl	1	CH_3	4-CH_3	$C_{15}H_{22}ClNO{\cdot}HCl$	180–181	C	+2.7
(*S*)-**2a**[d]	Cl	1	CH_3	4-CH_3	$C_{15}H_{22}ClNO{\cdot}HCl$	180–181	C	–2.7
(*R*)-**3a**	Cl	1	H	2-CH_3	$C_{14}H_{20}NClO{\cdot}HCl$	150–151	A	–7.7
(*S*)-**3a**	Cl	1	H	2-CH_3	$C_{14}H_{20}NClO{\cdot}HCl$	149–151	A	+7.5
4a	Cl	2	H	*cis*-2,6-di-CH_3	$C_{16}H_{24}NClO{\cdot}HCl$	156–157	D	
5a	Cl	1	H	*cis*-2,6-di-CH_3	$C_{15}H_{22}NClO{\cdot}HCl$	142–143	A	
6a	Cl	1	H	2,2,6,6-*tetra*-CH_3	$C_{17}H_{26}NClO{\cdot}HCl$	194–195	C	
1b	CH_3O	1	H	4-CH_3	$C_{15}H_{23}NO_2{\cdot}HCl$	154–156	C	
(*R*)-**2b**	CH_3O	1	CH_3	4-CH_3	$C_{16}H_{25}NO_2{\cdot}HCl$	151–153	D	+1.5
(*S*)-**2b**	CH_3O	1	CH_3	4-CH_3	$C_{16}H_{25}NO_2{\cdot}HCl$	151–152	D	–1.6
(*R*)-**3b**	CH_3O	1	H	2-CH_3	$C_{15}H_{23}NO_2{\cdot}HCl$	113–115	A	–5.4
(*S*)-**3b**	CH_3O	1	H	2-CH_3	$C_{15}H_{23}NO_2{\cdot}HCl$	112–114	A	+5.6
4b	CH_3O	2	H	*cis*-2,6-di-CH_3	$C_{17}H_{27}NO_2{\cdot}C_2H_2O_4$	98–99	B	
5b	CH_3O	1	H	*cis*-2,6-di-CH_3	$C_{16}H_{25}NO_2{\cdot}HCl$	131–132	B	
6b	CH_3O	1	H	2,2,6,6-tetra-CH_3	$C_{18}H_{29}NO_2{\cdot}HCl$	143–145	A	

[a]Elemental analyses for C, H and N were within ±0.4% of the theoretical values for the formulas given.
[b]Recrystallization solvent: A=AcOEt; B=AcOEt/Et_2O; C=AcOEt/abs. EtOH; D=Et_2O/abs. EtOH. [c](c=1.5 g/100 ml MeOH). [d]Formerly published data.[38]

Table 2. Binding Affinities and Selectivities.

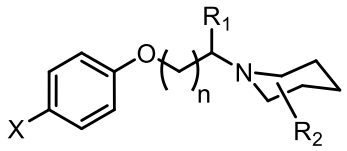

Compound	K_i ± SEM (nM)						
	X	**n**	**R_1**	**R_2**	σ_1	σ_2	Δ_8–Δ_7 SI
1a[a]	Cl	1	H	4-CH_3	0.86 ± 0.11	239 ± 15	3.70 ± 0.20
(*R*)-**2a**[a]	Cl	1	CH_3	4-CH_3	1.18 ± 0.05	52.3 ± 10.5	27.5 ± 7.1
(*S*)-**2a**[a]	Cl	1	CH_3	4-CH_3	0.34 ± 0.11	186 ± 12	3.73 ± 0.98
(*R*)-**3a**	Cl	1	H	2-CH_3	20.6 ± 1.6	77.8 ± 7.1	5.69 ± 1.31
(*S*)-**3a**	Cl	1	H	2-CH_3	16.6 ± 3.4	69.8 ± 13	2.27 ± 0.58
4a	Cl	2	H	*cis*-2,6-di-CH_3	4.43 ± 0.89	17.2 ± 0.2	6.56 ± 0.14
5a	Cl	1	H	*cis*-2,6-di-CH_3	59.4 ± 11.6	116 ± 28	4.55 ± 0.66
6a	Cl	1	H	2,2,6,6-tetra-CH_3	> 5000	411 ± 120	5.34 ± 0.65
1b	CH_3O	1	H	4-CH_3	0.89 ± 0.19	170 ± 30	86.8 ± 16.2
(*R*)-**2b**	CH_3O	1	CH_3	4-CH_3	1.16 ± 0.22	187 ± 3	161 ± 4
(*S*)-**2b**	CH_3O	1	CH_3	4-CH_3	1.49 ± 0.50	723 ± 87	168 ± 10
(*R*)-**3b**	CH_3O	1	H	2-CH_3	35.9 ± 7.0	300 ± 50	64.6 ± 0.5
(*S*)-**3b**	CH_3O	1	H	2-CH_3	43.4 ± 10.8	175 ± 2	68.5 ± 13.3
4b	CH_3O	2	H	*cis*-2,6-di-CH_3	23.5 ± 4.4	52.5 ± 7.3	11.9 ± 2.73
5b	CH_3O	1	H	*cis*-2,6-di-CH_3	379 ± 12	636 ± 68	31.3 ± 3.2
6b	CH_3O	1	H	2,2,6,6-tetra-CH_3	> 5000	809 ± 180	24.8 ± 3.4
(+)-pentazocine					3.93 ± 0.39		
DTG						29.5 ± 2.9	
(±)-ifenprodil							10.4 ± 1.9

[a]Formerly published data.[38]

Table 3. Cytotoxic activity of phenoxyalkypiperidines **1a,b-6a,b** in cancer cells.

Compounds	EC_{50} (μM)	
	C6	MCF7, SK-SY5Y, HepG2
1a, 1b	> 100	>100
2a-6a, 2b-6b	> 100	NT[a]

[a]NT: not tested

SCHEMES

Scheme 1.

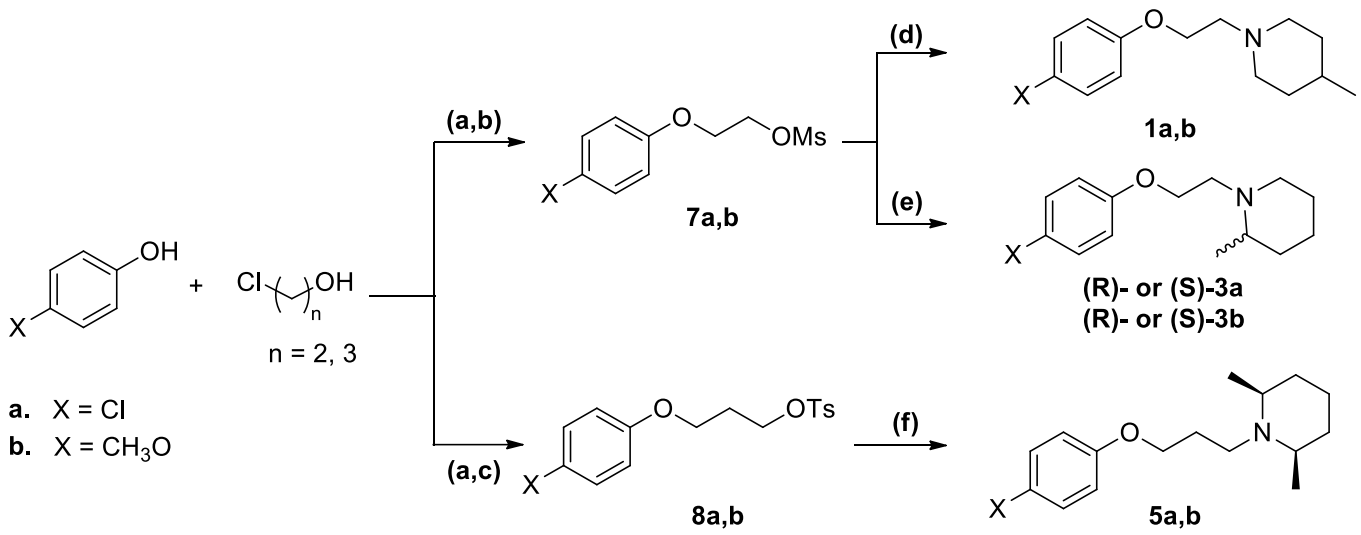

(a) 10% NaOH; (b) MsCl, Et_3N, dry CH_2Cl_2; (c) TsCl, Et_3N, dry CH_2Cl_2; (d) 4-Methylpiperidine, K_2CO_3, dry THF; HCl/Et_2O; (e) (*R*)- or (*S*)-2-Methylpiperidine, NaOH, H_2O/*i*-Pr; HCl/Et_2O; (f) *cis*-2,6-dimethylpiperidine, 1,2,2,6,6-pentamethylpiperidine, dry toluene; HCl/Et_2O or oxalic acid/EtOH.

Scheme 2.

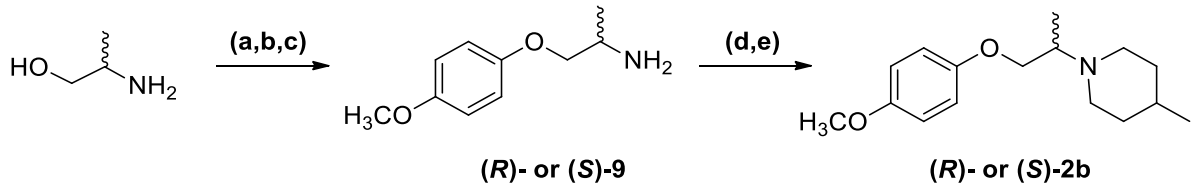

(a) Phthalic anhydride, Et_3N, toluene; (b) 4-methoxyphenol, Ph_3P, DIAD, dry THF; (c) 55% N_2H_4, AcOH/CH_3OH; (d) 3-Methylglutaric anhydride, dry THF; AcCl; (e) BMS, dry THF; HCl/Et_2O.

Scheme 3.

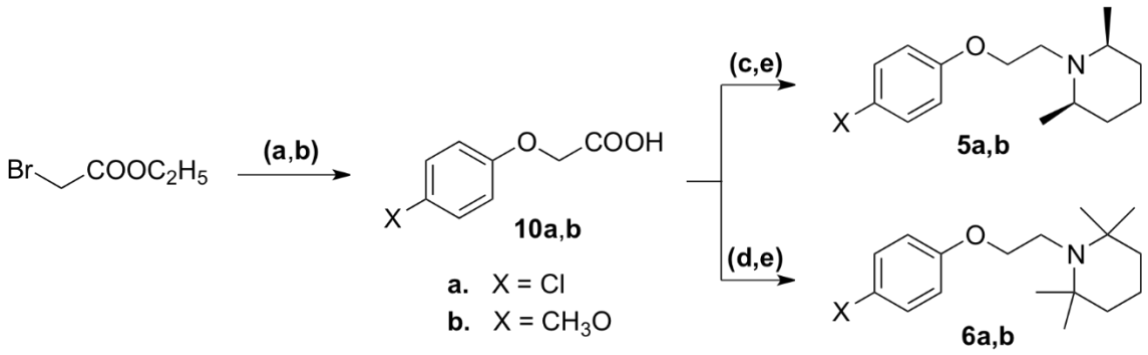

a) 4-Methoxyphenol, Na, abs. EtOH; (b) 1N NaOH/THF; (c) *cis*-2,6-dimethylpiperidine, DCC, dry CH_2Cl_2; (d) $SOCl_2$, 2,2,6,6-tetramethylpiperidine, Et_3N, dry CH_2Cl_2; (e) BMS, dry THF; HCl/Et_2O.

REFERENCES

(1) Martin, W. R.; Eades, C. G.; Thompson, J. A.; Huppler, R. E.; Gilbert, P. E. The Effects of Morphine- and Nalorphine-Like Drugs in the Nondependent and Morphine-Dependent Chronic Spinal Dog. *J. Pharmacol. Exp. Ther.* **1976**, *197*, 517–532.

(2) Kim, F. J.; Pasternak, G. W. Cloning the Sigma2 Receptor: Wandering 40 Years to Find an Identity. *Proc. Natl. Acad. Sci. U. S. A.* **2017**, *114*, 6888–6890.

(3) Hanner, M.; Moebus, F. F.; Flandorfer, A.; Knaus, H.-G.; Streissnig, J.; Kempner, E.; Glossman, H. Purification, Molecular Cloning, and Expression of the Mammalian Sigma$_1$-Binding Site. *Proc. Natl. Acad. Sci. U. S. A.* **1996**, *93*, 8072–8077.

(4) Schmidt, H. R.; Zheng, S.; Gurpinar, E.; Koehl, A.; Manglik, A.; Kruse, A. C. Crystal Structure of the Human σ_1 Receptor. *Nature* **2016**, *532*, 527–530.

(5) Xu, J.; Zeng, C.; Chu, W.; Pan, F.; Rothfuss, J. M.; Zhang, F.; Tu, Z.; Zhou, D.; Zeng, D.; Vangveravong, S.; Johnston, F.; Spitzer, D.; Chang, K. C.; Hotchkiss, R. S.; Hawkins, W. G.; Wheeler, K. T.; Mach, R. H. Identification of the PGRMC1 Protein Complex as the Putative Sigma-2 Receptor Binding Site. *Nat. Commun.* **2011**, *2*, 380.

(6) Chu, U. B.; Mavlyutov, T.; Chu, M.-L.; Yang, H.; Schulman, A.; Mesangeau, C.; McCurdy, C. R.; Guo, L.-W.; Ruoho, A. E. The Sigma-2 Receptor and Progesterone Receptor Membrane Component 1 are Different Binding Sites Derived From Independent Genes. *EBioMedicine* **2015**, *2*, 1806–1813.

(7) Abate, C.; Niso, M.; Infantino, V.; Menga, A.; Berardi, F. Elements in Support of the 'Non-Identity' of the PGRMC1 Protein with the σ2 Receptor. *Eur. J. Pharmacol.* **2015**, *758*, 16–23.

(8) Pati, M. L.; Groza, D.; Riganti, C.; Kopecka, J.; Niso, M.; Berardi, F.; Hager, S.; Heffeter, P.; Hirai, M.; Tsugawa, H.; Kabe, Y.; Suematsu, M.; Abate, C. Sigma-2 Receptor and Progesterone Receptor Membrane Component 1 (PGRMC1) Are Two Different Proteins: Proofs by Fluorescent Labeling and Binding of Sigma-2 Receptor Ligands to PGRMC1. *Pharmacol. Rep.* **2017**, *117*, 67–74.

(9) Alon, A.; Schmidt, H. R.; Wood, M. D.; Sahn, J. J.; Martin, S. F.; Kruse, A. C. Identification of the Gene That Codes for the σ2 Receptor. *Proc. Natl. Acad. Sci. U. S. A.* **2017**, *114*, 7160–7165.

(10) Abate, C.; Niso, M.; Berardi, F. Sigma-2 Receptor: Past, Present and Perspectives on Multiple Therapeutic Exploitations. *Future Med. Chem.* **2018**, *10*, 1997–2018.

(11) Izzo, N. J.; Colom-Cadena, M.; Riad, A. A.; Xu, J.; Singh, M.; Abate, C.; Cahill, M. A.; Spires-Jones, T. L.; Bowen, W. D.; Mach, R. M.; Catalano, S. M. Proceedings from the Fourth International Symposium on Sigma-2 Receptors: Role in Health and Disease. *eNeuro* **2020**, *7*, ENEURO.0317-20.2020.

(12) Schmidt, H. R.; Kruse, A. C. The Molecular Function of σ Receptors: Past, Present, and Future. *Trends Pharmacol. Sci.* **2019**, *40*, 636–654.

(13) Abatematteo, F.S.; Niso, M.; Lacivita, E.; Abate, C. *Molecules* **2021**, *26*, 3743.

(14) Schmidt, H. R.; Betz, R.; Dror, R. O.; Kruse, A. C. Structural Basis for σ_1 Receptor Ligand Recognition. *Nat. Struct. Mol. Biol.* **2018**, *25*, 981–987.

(15) Hayashi, T.; Su, T.-P. Sigma-1 Receptor Chaperones at the ER-Mitochondrion Interface Regulate Ca^{2+} Signaling and Cell Survival. *Cell* **2007**, *131*, 596–610.

(16) Hayashi, T.; Tsai, S.-Y.; Mori, T.; Fujimoto, M.; Su, T.-P. Targeting Ligand-Operated Chaperone Sigma-1 Receptors in the Treatment of Neuropsychiatric Disorders. *Expert Opin. Ther. Targets* **2011**, *15*, 557–577.

(17) Su, T.-P.; Su, T.-C.; Nakamura, Y.; Tsai, S.-Y. The Sigma-1 Receptor as a Pluripotent Modulator in Living Systems. *Trends Pharmacol. Sci.* **2016**, *37*, 262–278.

(18) Moritz, C.; Berardi, F.; Abate, C.; Peri, F. Live Imaging Reveals a New Role for the Sigma-1 (σ_1) Receptor in Allowing Microglia to Leave Brain Injuries. *Neurosci. Lett.* **2015**, *591*, 13–18.

(19) Crouzier, L.; Couly, S.; Roques, C.; Peter, C.; Belkhiter, R.; Jaquemin, M. A.; Bonetto, A.; Delprat, B.; Maurice, T. Sigma-1 (σ_1) Receptor Activity is Necessary for Physiological Brain Plasticity in Mice. *Eur. Neuropsychopharmacol.* **2020**, *39*, 29–45.
(20) Moriguchi, S.; Shinoda, Y.; Yamamoto, Y.; Sasaki, Y.; Miyajima, K.; Tagashira, H.; Fukunaga, K. Stimulation of the Sigma-1 Receptor by DHEA Enhances Synaptic Efficacy and Neurogenesis in the Hippocampal Dentate Gyrus of Olfactory Bulbectomized Mice. *PLoS One* **2013**, *8*, e60863.
(21) Ruscher, K.; Shamloo, M.; Rickhag, M.; Ladunga, I.; Soriano, L.; Gisselsson, L.; Toresson, H.; Ruslim-Litrus, L.; Oksenberg, D.; Urfer, R.; Johansson, B. B.; Nikolich, K.; Wieloch, T. The Sigma-1 Receptor Enhances Brain Plasticity and Functional Recovery after Experimental Stroke. *Brain* **2011**, *134*, 732–746.
(22) Snyder, M. A.; McCann, K.; Lalande, M. J.; Thivierge, J.-P.; Bergeron, R. Sigma Receptor Type 1 Knockout Mice Show a Mild Deficit in Plasticity but No Significant Change in Synaptic Transmission in the CA1 Region of the Hippocampus. *J. Neurochem.* **2016**, *138*, 700–709.
(23) Maurice, T.; Goguadze, N. Role of σ_1 Receptors in Learning and Memory and Alzheimer's Disease-Type Dementia. *Adv. Exp. Med. Biol.* **2017**, *964*, 213–233.
(24) Maurice, T.; Goguadze, N. Sigma-1 (σ_1) Receptor in Memory and Neurodegenerative Diseases. *Handb. Exp. Pharmacol.* **2017**, *244*, 81–108.
(25) Geva, M.; Kusko, R.; Soares, H.; Fowler, K. D.; Birnberg, T.; Barash, S.; Merenlender-Wagner, A.; Fine, T.; Lysaght, A.; Weiner, B.; Cha, Y.; Kolitz, S.; Towfic, F.; Orbach, A.; Laufer, R.; Zeskind, B.; Grossman, I.; Hayden, M. R. Pridopidine Activates Neuroprotective Pathways Impaired in Huntington Disease. *Hum. Mol. Genet.* **2016**, *25*, 3975–3987.
(26) Ionescu, A.; Gradus, T.; Altman, T.; Maimon, R.; Avraham, N. S.; Geva, M.; Hayden, M.; Perlson, E. Targeting the Sigma-1 Receptor via Pridopidine Ameliorates Central Features of ALS Pathology in a $SOD1^{G93A}$ Model. *Cell Death Dis.* **2019**, *10*, 210.
(27) Maurice, T. Bi-Phasic Dose Response in the Preclinical and Clinical Developments of Sigma-1 Receptor Ligands for the Treatment of Neurodegenerative Disorders. *Expert Opin. Drug Discovery* **2021**, *16*, 373–389.
(28) McGarry, A.; Leinonen, M.; Kieburtz, K.; Geva, M.; Olanow, C. W.; Hayden, M. R. Effects of Pridopidine on Functional Capacity in Early-Stage Participants from the PRIDE-HD Study. *Journal of Huntington's Disease* **2020**, *9*, 371–380.
(29) Shenkman, M.; Geva, M.; Gershoni-Emek, N.; Hayden, M. R.; Lederkremer, G. Z. Pridopidine Reduces Mutant Huntingtin-Induced Endoplasmic Reticulum Stress by Modulation of the Sigma-1 Receptor. *J. Neurochem.* **2021**, *158*, 467-481
(30) Fallica, A. N.; Pittalà, V.; Modica, M. N.; Salerno, L.; Romeo, G.; Marrazzo, A.; Helal, M. A.; Intagliata, S. Recent Advances in the Development of Sigma Receptor Ligands as Cytotoxic Agents: A Medicinal Chemistry Perspective. *J. Med. Chem.* **2021**, *64*, 7926–7962.
(31) Gordon, D. E.; Hiatt, J.; Bouhaddou, M.; Rezelj, V. V.; Ulferts, S.; Braberg, H.; Jureka, A. S.; Obernier, K.; Guo, J. Z.; Batra, J.; Kaake, R. M.; Weckstein, A. R.; Owens, T. W.; Gupta, M.; Pourmal, S.; Titus, E. W.; Cakir, M.; Soucheray, M.; McGregor, M.; Cakir, Z.; Jang, G.; O'Meara, M. J.; Tummino, T. A.; Zhang, Z.; Foussard, H.; Rojc, A.; Zhou, Y.; Kuchenov, D.; Hüttenhain, R.; Xu, J.; Eckhardt, M.; Swaney, D. L.; Fabius, J. M.; Ummadi, M.; Tutuncuoglu, B.; Rathore, U.; Modak, M.; Haas, P.; Haas, K. M.; Naing, Z. Z. C.; Pulido, E. H.; Shi, Y.; Barrio-Hernandez, I.; Memon, D.; Petsalaki, E.; Dunham, A.; Correa Marrero, M.; Burke, D.; Koh, C.; Vallet, T.; Silvas, J. A.; Azumaya, C. M.; Billesbølle, C.; Brilot, A. F.; Campbell, M. G.; Diallo, A.; Dickinson, M. S.; Diwanji, D.; Herrera, N.; Hoppe, N.; Kratochvil, H. T.; Liu, Y.; Merz, G. E.; Moritz, M.; Nguyen, H. C.; Nowotny, C.; Puchades, C.; Rizo, A. N.; Schulze-Gahmen, U.; Smith, A. M.; Sun, M.; Young, I. D.; Zhao, J.; Asarnow, D.; Biel, J.; Bowen, A.; Braxton, J. R.; Chen, J.; Chio, C. M.; Chio, U. S.; Deshpande, I.; Doan, L.; Faust, B.; Flores, S.; Jin, M.; Kim, K.; Lam, V. L.; Li, F.; Li, J.; Li, Y.-L.; Li, Y.; Liu, X.; Lo, M.; Lopez, K. E.; Melo, A. A.; Moss, F. R., III; Nguyen, P.; Paulino, J.; Pawar, K. I.; Peters, J. K.; Pospiech, T. H., Jr.; Safari, M.; Sangwan, S.; Schaefer, K.; Thomas, P. V.; Thwin,

A. C.; Trenker, R.; Tse, E.; Tsui, T. K. M.; Wang, F.; Whitis, N.; Yu, Z.; Zhang, K.; Zhang, Y.; Zhou, F.; Saltzberg, D.; QCRG Structural Biology Consortium; Hodder, A. J.; Shun-Shion, A. S.; Williams, D. M.; White, K. M.; Rosales, R.; Kehrer, T.; Miorin, L.; Moreno, E.; Patel, A. H.; Rihn, S.; Khalid, M. M.; Vallejo-Gracia, A.; Fozouni, P.; Simoneau, C. R.; Roth, T. L.; Wu, D.; Karim, M. A.; Ghoussaini, M.; Dunham, I.; Berardi, F.; Weigang, S.; Chazal, M.; Park, J.; Logue, J.; McGrath, M.; Weston, S.; Haupt, R.; Hastie, C. J.; Elliott, M.; Brown, F.; Burness, K. A.; Reid, E.; Dorward, M.; Johnson, C.; Wilkinson, S. G.; Geyer, A.; Giesel, D. M.; Baillie, C.; Raggett, S.; Leech, H.; Toth, R.; Goodman, N.; Keough, K. C.; Lind, A. L.; Zoonomia Consortium; Klesh, R. J.; Hemphill, K. R.; Carlson-Stevermer, J.; Oki, J.; Holden, K.; Maures, T.; Pollard, K. S.; Sali, A.; Agard, D. A.; Cheng, Y.; Fraser, J. S.; Frost, A.; Jura, N.; Kortemme, T.; Manglik, A.; Southworth, D. R.; Stroud, R. M.; Alessi, D. R.; Davies, P.; Frieman, M. B.; Ideker, T.; Abate, C.; Jouvenet, N.; Kochs, G.; Shoichet, B.; Ott, M.; Palmarini, M.; Shokat, K. M.; García-Sastre, A.; Rassen, J. A.; Grosse, R.; Rosenberg, O. S.; Verba, K. A.; Basler, C. F.; Vignuzzi, M.; Peden, A. A.; Beltrao, P.; Krogan, N. J. Comparative Host-Coronavirus Protein Interaction Networks Reveal Pan-Viral Disease Mechanisms. *Science* **2020**, *370*, eabe9403.

(32) Gordon, D. E.; Jang, G. M.; Bouhaddou, M.; Xu, J.; Obernier, K.; White, K. M.; O'Meara, M. J.; Rezelj, V. V.; Guo, J. Z.; Swaney, D. L.; Tummino, T. A.; Hüttenhain, R.; Kaake, R. M.; Richards, A. L.; Tutuncuoglu, B.; Foussard, H.; Batra, J.; Haas, K.; Modak, M.; Kim, M.; Haas, P.; Polacco, B. J.; Braberg, H.; Fabius, J. M.; Eckhardt, M.; Soucheray, M.; Bennett, M. J.; Cakir, M.; McGregor, M. J.; Li, Q.; Meyer, B.; Roesch, F.; Vallet, T.; Mac Kain, A.; Miorin, L.; Moreno, E.; Naing, Z. Z. C.; Zhou, Y.; Peng, S.; Shi, Y.; Zhang, Z.; Shen, W.; Kirby, I. T.; Melnyk, J. E.; Chorba, J. S.; Lou, K.; Dai, S. A.; Barrio-Hernandez, I.; Memon, D.; Hernandez-Armenta, C.; Lyu, J.; Mathy, C. J. P.; Perica, T.; Pilla, K. B.; Ganesan, S. J.; Saltzberg, D. J.; Ramachandran, R.; Liu, X.; Rosenthal, S. B.; Calviello, L.; Venkataramanan, S.; Liboy-Lugo, J.; Lin, Y.; Huang, X.-P.; Liu, Y.; Wankowicz, S. A.; Bohn, M.; Safari, M.; Ugur, F. S.; Koh, C.; Savar, N. S.; Tran, Q. D.; Shengjuler, D.; Fletcher, S. J.; O'Neal, M. C.; Cai, Y.; Chang, J. C. J.; Broadhurst, D. J.; Klippsten, S.; Sharp, P. P.; Wenzell, N. A.; Kuzuoglu-Ozturk, D.; Wang, H.-Y.; Trenker, R.; Young, J. M.; Cavero, D. A.; Hiatt, J.; Roth, T. L.; Rathore, U.; Subramanian, A.; Noack, J.; Hubert, M.; Stroud, R. M.; Frankel, A. D.; Rosenberg, O. S.; Verba, K. A.; Agard, D. A.; Ott, M.; Emerman, M.; Jura, N.; von Zastrow, M.; Verdin, E.; Ashworth, A.; Schwartz, O.; d'Enfert, C.; Mukherjee, S.; Jacobson, M.; Malik, M. S.; Fujimori, D. J.; Ideker, T.; Craik, C. S.; Floor, S. N.; Fraser, J. S.; Gross, J. D.; Sali, A.; Roth, B. L.; Ruggero, D.; Taunton, J.; Kortemme, T.; Beltrao, P.; Vignuzzi, M.; García-Sastre, A.; Shokat, K. M.; Shoichet, B. K.; Krogan, N. J. A SARS-CoV-2 Protein Interaction Map Reveals Targets for Drug Repurposing. *Nature* **2020**, *583*, 459–468.

(33) Vela, J. M. Repurposing Sigma-1 Receptor Ligands for COVID-19 Therapy? *Front. Pharmacol.* **2020**, *11*, 582310.

(34) Tummino, T.A.; Rezelj, V.V.; Fischer, B.; Fischer, A.; O'Meara, M.J.; Monel, B.; Vallet, T.;White, K.M.; Zhang, Z.; Alon, A.; Schadt, H.; O'Donnell, H.R.; Lyu, J.; Rosales, R.; McGovern, B.L.; Rathnasinghe, R.; Jangra, S.; Schotsaert, M.; Galerneau, J.; Krogan, N.J.; Urban, L.; Shokat, K.M.; Kruse, A.C.; Garcia-Sastre, A.; Schwartz, O.; Moretti, R.; Vignuzzi, M.; Pognan, F.; Shoichet, B.K. Drug-induced phospholipidosis confounds drug repurposing for SARS-CoV-2. *Science* **2021**, eabi4708.

(35) Abatematteo, F. S.; Niso, M.; Contino, M.; Leopoldo, M.; Abate, C. Multi-Target Directed Ligands (MTDLs) Binding the σ_1 Receptor as Promising Therapeutics: State of the Art and Perspectives. *Int. J. Mol. Sci.* **2021**, *22*, 6359.

(36) García, M.; Virgili, M.; Alonso, M.; Alegret, C.; Farran, J.; Fernández, B.; Bordas, M.; Pascual, R.; Burgueño, J.; Vidal-Torres, A.; Fernández de Henestrosa, A. R.; Ayet, E.; Merlos, M.; Vela, J. M.; Plata-Salamán, C. R.; Almansa, C. Discovery of EST73502, a Dual μ-Opioid Receptor Agonist and σ_1 Receptor Antagonist Clinical Candidate for the Treatment of Pain. *J. Med. Chem.* **2020**, *63*, 15508–15526.

(37) Berardi, F.; Ferorelli, S.; Abate, C.; Pedone, M. P.; Colabufo, N. A.; Contino, M.; Perrone, R. Methyl Substitution on the Piperidine Ring of *N*-[ω-(6-Methoxynaphthalen-1-yl)alkyl] Derivatives as a Probe for Selective Binding and Activity at the σ_1 Receptor. *J. Med. Chem.* **2005**, *48*, 8237–8244.
(38) Berardi, F.; Loiodice, F.; Fracchiolla, G.; Colabufo, N. A.; Perrone, R.; Tortorella, V. Synthesis of Chiral 1-[ω-(4-Chlorophenoxy)alkyl]-4-methylpiperidines and Their Biological Evaluation at σ_1, σ_2, and Sterol Δ_8-Δ_7 Isomerase Sites. *J. Med. Chem.* **2003**, *46*, 2117–2124.
(39) Niso, M.; Abate, C.; Ferorelli, S.; Cassano, G.; Gasparre, G.; Perrone, R.; Berardi, F. Investigation of σ Receptors Agonist/Antagonist Activity through *N*-(6-Methoxytetralin-1-yl)- and *N*-(6-Methoxynaphthalen-1-yl)alkyl Derivatives of Polymethylpiperidines. *Bioorg. Med. Chem.* **2013**, *21*, 1865–1869.
(40) Yano, H.; Bonifazi, A.; Xu, M.; Guthrie, D. A.; Schneck, S. N.; Abramyan, A. M.; Fant, A. D.; Hong, W. C.; Newman, A. H.; Shi, L. Pharmacological Profiling of Sigma 1 Receptor Ligands by Novel Receptor Homomer Assays. *Neuropharmacology* **2018**, *133*, 264–275.
(41) Niso, M.; Mosier, P. D.; Marottoli, R.; Ferorelli, S.; Cassano, G.; Gasparre, G.; Leopoldo, M.; Berardi, F.; Abate, C. High Affinity and Selectivity Sigma-1 (σ_1) Receptor Ligands Based on the σ_1 Antagonist PB212. *Future Med. Chem.* **2019**, *11*, 2547–2562.
(42) Moebius, F. F.; Fitzky, B. U.; Wietzorrek, G.; Haidekker, A.; Eder, A.; Glossman, H. Cloning of an Emopamil-Binding Protein (EBP)-Like Protein that Lacks Sterol Δ^8-Δ^7 Isomerase Activity. *Biochem. J.* **2003**, *374*, 229–237.
(43) Maurice, T.; Hiramatsu, M.; Itoh, J.; Kameyama, T.; Hasegawa, T.; Nabeshima, T. Behavioral Evidence for a Modulating Role of σ Ligands in Memory Processes. I. Attenuation of Dizocilpine (MK-801)-Induced Amnesia. *Brain Res.* **1994**, *647*, 44–56.
(44) Maurice, T.; Phan, V.-L.; Privat, A. The Anti-Amnesic Effects of Sigma$_1$ (σ_1) Receptor Agonists Confirmed by *in vivo* Antisense Strategy in the Mouse. *Brain Res.* **2001**, *898*, 113–121.
(45) Maurice, T.; Su, T-P.; Parish, D.W.; Nabeshima, T.; Privat, A. PRE-084, a sigma selective PCP derivative, attenuates MK-801-induced impairment of learning in mice. *Pharmacol Biochem Behav*. **1994**, *49*, 859-69.
(46) Rauk, A.; Tavares, F.D.; Khan, M. A.; Borkent, A. J.; Olson, J. F. Conformational analysis of chiral hindered amides. Can. J. Chem. **1983**, 61, 2572–2580.
(47) Insaf, S. S.; Witiak, D. T. Facile Non-Racemizing Route for the N-Alkylation of Hindered Secondary Amines. Synthesis, **1999**, 3, 435–440.
(48) Matsumoto, R. R.; Bowen, W. D.; Tom, M. A.; Vo, V. N.; Truong, D. D.; de Costa, B. R. Characterization of Two Novel s Receptor Ligands: Antidystonic Effects in Rats Suggest σ Receptor Antagonism. *Eur. J. Pharmacol.* **1995**, *280*, 301–310.
(49) Berardi, F.; Abate, C.; Ferorelli, S.; de Robertis, A. F.; Leopoldo, M.; Colabufo, N. A.; Niso, M.; Perrone, R. Novel 4-(4-Aryl)cyclohexyl-1-(2-pyridyl)piperazines as Δ_8–Δ_7 Sterol Isomerase (Emopamil Binding Protein) Selective Ligands with Antiproliferative Activity. *J. Med. Chem.* **2008**, *51*, 7523–7531.
(50) Pati, M.L.; Hornick, J.R.; Niso, M.; Berardi, F.; Spitzer, D.; Abate, C.; Hawkins, W. Sigma-2 receptor agonist derivatives of 1-Cyclohexyl-4-[3-(5-methoxy-1,2,3,4-tetrahydronaphthalen-1-yl)propyl]piperazine (PB28) induce cell death via mitochondrial superoxide production and caspase activation in pancreatic cancer. *BMC Cancer*, **2017**, *17*, 51
(51) Kilkenny, C.; Browne, W.; Cuthill, I. C.; Emerson, M.; Altman, D. G. Animal Research: Reporting *in vivo* Experiments: The ARRIVE Guidelines. *Br. J. Pharmacol.* **2010**, *160*, 1577–1579.
(52) Maurice, T.; Lockhart, B. P.; Privat, A. Amnesia Induced in Mice by Centrally Administered β-Amyloid Peptides Involves Cholinergic Dysfunction. *Brain Res.* **1996**, *706*, 181–193.
(53) Meunier, J.; Ieni, J.; Maurice, T. The Anti-Amnesic and Neuroprotective Effects of Donepezil against Amyloid $\beta_{25\text{-}35}$ Peptide-Induced Toxicity in Mice Involve an Interaction with the σ_1 Receptor. *Br. J. Pharmacol.* **2006**, *149*, 998–1012.
(54) Meunier, J.; Villard, V.; Givalois, L.; Maurice, T. The γ-Secretase Inhibitor 2-[(1*R*)-1-[(4-Chlorophenyl)sulfonyl](2,5-difluorophenyl)amino]ethyl-5-fluorobenzenebutanoic Acid (BMS-

299897) Alleviates $A\beta_{1-42}$ Seeding and Short-Term Memory Deficits in the $A\beta_{25-35}$ Mouse Model of Alzheimer's Disease. *Eur. J. Pharmacol.* **2013**, *698*, 193–199.
(55) Villard, V.; Espallergues, J.; Keller, E.; Alkam, T.; Nitta, A.; Yamada, K.; Nabeshima, T.; Vamvakides, A.; Maurice, T. Antiamnesic and Neuroprotective Effects of the Aminotetrahydrofuran Derivative ANAVEX1-41 Against Amyloid β_{25-35}-Induced Toxicity in Mice. *Neuropsychopharmacology* **2009**, *34*, 1552–1566.
(56) Villard, V.; Espallergues, J.; Keller, E.; Vamvakides, A.; Maurice, T. Anti-Amnesic and Neuroprotective Potentials of the Mixed Muscarinic Receptor/$Sigma_1$ (σ_1) Ligand ANAVEX2-73, a Novel Aminotetrahydrofuran Derivative. *J. Psychopharmacol.* **2011**, *25*, 1101–1117.

Table of Content Graphic

Development of Novel Phenoxyalkylpiperidines as High-Affinity Sigma-1 (σ_1) Receptor Ligands with Potent Anti-Amnesic Effect

Francesca S. Abatematteo, Philip D. Mosier, Mauro Niso, Leonardo Brunetti, Francesco Berardi, Fulvio Loiodice, Marialessandra Contino, Benjamin Delprat, Maurice Tangui, Antonio Laghezza* and Carmen Abate*